LEVEL II

12

RADC-TR-81-98
Final Technical Report
June 1981

STUDY OF MICROSTRIP ANTENNA ELEMENTS, ARRAYS, FEEDS, LOSSES AND APPLICATIONS

University of Illinois at Urbana-Champaign

Y. T. Lo
W. F. Richards
P. S. Simon
J. E. Brewer
C. P. Yuan

ROME AIR DEVELOPMENT CENTER
Air Force Systems Command
Griffiss Air Force Base, New York 13441

This report has been reviewed by the RADC Public Affairs Office (PA) and is releasable to the National Technical Information Service (NTIS). At NTIS it will be releasable to the general public, including foreign nations.

RADC-TR-81-98 has been reviewed and is approved for publication.

APPROVED: John A. Strom

JOHN A. STROM
Project Engineer

APPROVED: Allan C. Schell

ALLAN C. SCHELL
Chief, Electromagnetic Sciences Division

FOR THE COMMANDER: John P. Huss

JOHN P. HUSS
Acting Chief, Plans Office

If your address has changed or if you wish to be removed from the RADC mailing list, or if the addressee is no longer employed by your organization, please notify RADC (EEAA) Hanscom AFB MA 01731. This will assist us in maintaining a current mailing list.

Do not return this copy. Retain or destroy.

UNCLASSIFIED

SECURITY CLASSIFICATION OF THIS PAGE (When Data Entered)

REPORT DOCUMENTATION PAGE

READ INSTRUCTIONS BEFORE COMPLETING FORM

1. REPORT NUMBER: RADC-TR-81-98	2. GOVT ACCESSION NO: AD-A104 493
3. RECIPIENT'S CATALOG NUMBER:	
4. TITLE (and Subtitle): STUDY OF MICROSTRIP ANTENNA ELEMENTS, ARRAYS, FEEDS, LOSSES, AND APPLICATIONS	5. TYPE OF REPORT & PERIOD COVERED: Final Technical Report
	6. PERFORMING ORG. REPORT NUMBER: EM 81-2, UILU-81-2539
7. AUTHOR(s): Y. T. Lo, J. E. Brewer, W. F. Richards, C. P. Yuan, P. S. Simon	8. CONTRACT OR GRANT NUMBER(s): F19628-78-C-0025
9. PERFORMING ORGANIZATION NAME AND ADDRESS: University of Illinois at Urbana-Champaign, Dept of Electrical Engineering/Electromagnetics Lab, Urbana IL 61801	10. PROGRAM ELEMENT, PROJECT, TASK AREA & WORK UNIT NUMBERS: 61102F, 2305J323
11. CONTROLLING OFFICE NAME AND ADDRESS: Deputy for Electronic Technology (RADC/EEAA), Hanscom AFB MA 01731	12. REPORT DATE: June 1981
	13. NUMBER OF PAGES: 86
14. MONITORING AGENCY NAME & ADDRESS (if different from Controlling Office): Same	15. SECURITY CLASS. (of this report): UNCLASSIFIED
	15a. DECLASSIFICATION/DOWNGRADING SCHEDULE: N/A

16. DISTRIBUTION STATEMENT (of this Report)

Approved for public release; distribution unlimited.

17. DISTRIBUTION STATEMENT (of the abstract entered in Block 20, if different from Report)

Same

18. SUPPLEMENTARY NOTES

RADC Project Engineers: John A. Strom and Nicholas Kernweis (RADC/EEAA)

19. KEY WORDS (Continue on reverse side if necessary and identify by block number)

Microstrip Antennas, Excitation of Cavity and Input Impedance, Multiport Microstrip Antennas, Circularly Polarized Microstrip Antennas, Circuit Representation of Microstrip Antennas, Microstrip Antenna Arrays, Microstrip Antenna Losses

20. ABSTRACT (Continue on reverse side if necessary and identify by block number)

In this report, a few highlights of the work performed under the contract F19628-78-C-0025 are summarized. Details of some of the findings have been published in four Interim Reports. But for the practical engineers whose interests are mainly in design concept and method, only a few simple formulas are summarized here. Some other findings which have not been reported previously are discussed in some detail.

Continued

DD FORM 1 JAN 73 1473 EDITION OF 1 NOV 65 IS OBSOLETE

UNCLASSIFIED

SECURITY CLASSIFICATION OF THIS PAGE (When Data Entered)

Item 20 (Continued)

Briefly, the cavity model theory developed previously is refined so that it can be applied even if the dominant mode is not strongly excited. This improved theory has been tested for microstrip antennas of two typical geometries: rectangles and circular disks. In both cases, the agreement with the measured results is found to be remarkable.

It is well-known that a microstrip antenna can produce circularly polarized (CP) waves with only a single input post and no phasing networks. But, so far, the required dimensions of the antenna are determined by a painstaking trial-and-error method, either by experiment or with a computer. Since CP operation is possible only for a small portion of the already small bandwidth of the microstrip antenna, the search for those critical dimensions of the aforementioned method is clearly time-consuming and costly. From our improved theory, a surprisingly simple formula is derived to obtain the necessary dimensions of a nearly square CP patch antenna. The accuracy of this formula is verified experimentally with almost perfect agreement. This work is extended to elliptical CP patch antennas and again the same close agreement with the experiment is observed.

Since thin microstrip antennas are inherently narrow band, it is important to have a simple means for tuning the antenna over a wide range. Based on the cavity-model theory, one can expect that the antenna could be tuned like a cavity. Some workers have demonstrated experimentally the tuning with a shorting post in the patch. It is desirable to have a theory which can predict the exact post location for a given operating frequency. To this end, our multiport theory is extended so that a simple algorithm can be applied to a wide frequency range, covering the resonant frequencies of several modes. Using this extended theory, the operating frequencies for many post locations are computed and found to agree with the measured results within a fraction of one percent. In fact, it is believed that the theory can be improved even further. It is also shown that CP can also be obtained by placing a post in a square patch. Again, the theoretical and experimental results are in almost perfect agreement.

Most microstrip antenna studies so far are characterized by a simply connected region in geometry. Since our theory implies that it is mainly the equivalent magnetic current along the patch boundary that radiates, the question has been raised as to whether patches bounded by two or more closed curves would have different radiation characteristics. To obtain a quick answer to this question, annulus and "quadrulus" (i.e., a rectangle with a concentric rectangular region removed) patches are investigated. No significant difference is observed except, as expected, for the change in resonant frequencies and cross-polarized component patterns.

Previous investigations show that the impedance locus of a microstrip antenna can be varied over a wide range simply by changing the coaxial feed location in the patch, thus providing a simple means for impedance matching. However, the use of cable feed increases the manufacturing complexity since it cannot be produced simply by "printed circuit" technique. To alleviate this difficulty, the method of using a stripline feed through a slit cut in the patch is investigated. Similar impedance variation is obtained.

In a microstrip antenna, there is a dielectric loss in the substrate and copper loss in the cladding. Manufacturers usually provide the value of dielectric loss tangent with no mention of the copper loss. But in the manufacturing process, the copper-to-dielectric interface is physically

Item 20 (Continued)

and chemically treated, and as a result, there is a profound effect on the copper loss. Conventional methods of measurement cannot determine this copper loss without altering the surface condition. Therefore, a new technique is developed which can separate the two losses in measurement without physically separating the two materials. The result shows that the loss in copper cladding is substantially higher than what would be computed by using the published conductivity value for pure copper.

The most challenging problem in microstrip antennas is how to broaden the bandwidth. The method of stacking two patches tuned to slightly different frequencies is not very successful because the small gain in bandwidth could have been achieved much more simply by using a single patch of double thickness, since both bandwidth and efficiency increase with the substrate thickness. But increasing the thickness is not desirable in many applications. Thus a planar array of two thin microstrip elements of slightly different dimensions is investigated. Using the network representation for the elements, an efficient algorithm for the array is developed to search for an "optimum" design in the sense that the bandwidth is largest for a given SWR and simultaneously maintaining a stable pattern. Unfortunately, the bandwidth gained is not appreciable. But the algorithm can be used to design an array for dual-frequency operation.

For a very thick microstrip antenna, or one operating at very high frequencies, the cavity model may no longer be valid. For this case, a rigorous theory is formulated in terms of integral equations. Because of the numerical complexity, only some preliminary work is performed up to this point.

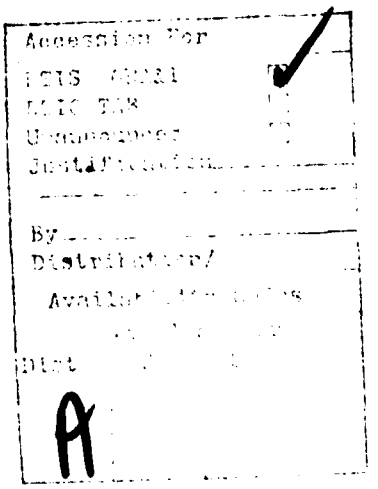

TABLE OF CONTENTS

LIST OF FIGURES

I. INTRODUCTION

This report covers most of the work performed under the Contract F19628-78-C-0025. During the course of the investigation activities in each quarter have been periodically reported while the accomplishment of each major task has been published in four Interim Reports. Also reported is a complete and efficient computer program for evaluating all antenna characteristics, including input impedance locus, radiation patterns, power lost and radiated, Q-factor, and efficiency, of the widely used rectangular microstrip antenna with a single input port, or two input ports, or one input port and the other arbitrarily loaded. In this final report, for completeness, a few highlights (which may be useful for the designers) in the four Interim Reports will be summarized, while some other findings which have not been reported will be discussed in some detail.

It is well-known that an elliptical patch element, like a nearly square patch, if designed and fed properly, can radiate circularly polarized waves. Hitherto, they are determined only by the painstaking and time-consuming trial and error method [12]. Recently, Shen [9] uses the elliptical cylinder functions pertaining to the geometry for the modal expansion of the field, and to avoid the computational complication he resorts to the approximations for those functions, when the axial ratio is small. From this a numerical search is then made for the best axial ratio (actually, in his paper the best operating frequency is sought for a given axial ratio). Clearly, this method of computer searching is also time-consuming and costly. Using a perturbation technique in conjunction with the simple theory we developed previously, the required axial ratio can readily be determined, and, in fact, it is found to be in almost perfect agreement with the experiment. This is discussed in Section III. From this study, some general conclusion will be made.

Schaubert, et. al [15] reported that a microstrip antenna, as a cavity, can be tuned over a wide frequency band by placing posts in the patch, and, in fact, circular polarization can be obtained in a similar manner. But their work is mainly experimental on a trial and error basis. For an analytic solution to this problem, the multiport theory developed earlier [6] can be applied. However, in all the applications studied previously, only a narrow band in the vicinity of the resonant frequency of any exciting mode is of concern, while in this application, an efficient wide band algorithm is needed. This is discussed in Section IV.

Most patch antennas investigated so far are bounded by a single closed curve. Since, according to the cavity model theory, it is the equivalent magnetic current along the patch perimeter that radiates, question has been raised as to whether patches bounded by two or more closed curves would have different radiation characteristics. To answer this question, patch antennas of two different geometries are investigated. The first is an annulus which can be analyzed theoretically, and the other is a rectangular patch with a concentric similar rectangular region removed. The latter shall be, for convenience, called "Quadrulus." The results show that so far as the radiation pattern, the impedance characteristics, and the bandwidth are concerned, they are essentially the same as that of the patches without holes. The most noticable difference is the change in resonant frequency, and in some cases, the magnitude and the pattern of cross-polarized field components. This is reported in Section V.

One interesting property of the patch antenna is its built-in mechanism for impedance matching. As shown in our previous investigation, this is accomplished by feeding the patch internally with a coaxial cable. But in so doing, the antenna is not strictly monolithic, so that the advantage in manufacture by using the printed circuit technique is lost. For this reason an experimental program is launched to investigate whether the cable-feed inside

the patch could be replaced by a stripline-feed through a slot cut in the patch. Indeed, similar impedance variation is obtained. This is discussed in Section VI.

The rigorous theory of microstrip antenna has been considered off and on during the last part of the contract period. The purpose is to prepare for a major investigation in the next contract in which the applications of microstrip antennas at much higher frequency will be studied. Since this problem is closely parallel to that of an infinite periodic array of patch elements, both problems are examined simultaneously. Because of the numerical complication, only formulation is reported here.

II. AN IMPROVED THEORY

Analytic works on microstrip antennas can be grouped into four different approaches. The first due to Munson [1] and his followers [2] is based on a transmission line model, in which two opposite sides of a rectangular patch are considered as the radiating edges and they are connected by a low impedance stripline, namely the patch. They use the impedance of a semi-infinite parallel-plate guide derived approximately by Harrington [3] as the impedance of each edge. Clearly many questions could be raised about this approach since each edge is not geometrically identical to the parallel-plate guide in many respects. Furthermore, when a feed is connected to one edge, as is usually the case, exactly how the impedance looking into the feed line is related to the edge impedance is open to question. Obviously, this approach is difficult, if not impossible, to apply for any general feed location in the patch, and also cannot be applied to geometrics other than rectangle. It is therefore not surprising to see much disagreement between its predicted and measured impedance loci except for some special cases.

A second approach is purely numerical by modeling the antenna as a grid of wires [4]. While the method seems to give reasonably good results, it is costly and provides little understanding of the operation mechanism of the antenna.

Taking advantage of the thinness of the antenna, a third approach is made by modeling the antenna as a cavity [5]. It is based on the assumption that the field structure under the patch is not much different from that of a corresponding cavity, which is made of the patch, the ground plane, and a magnetic wall along the perimeter. Once this is accepted, the usual analytic procedure can be followed for a solution. First, the field is expanded in terms of

modes and second from the expansion one can find the stored energies, the dielectric and copper losses, as well as the radiated power. From all these quantities the input impedance can be computed from any one of the three formulas: (a) admittance in terms of total real power loss, stored energy and input voltage, (b) impedance in terms of total real power loss, stored energy and input current, and (c) impedance as the ratio of input voltage to input current. In the theory developed previously [5] computations based on (a) have given results in close agreement with the measured. However for the feed location where the dominant modes are not strongly excited, not only erroneous results are obtained, but the computations based on the above three formulas give inconsistent results. An improved theory is therefore developed in conjunction with a highly efficient numerical method [6]. It yields accurate results for any feed location and also for several critical applications. This approach is simple and elegant, but also provides much physical insights into the mechanism of the antenna operation, that lead to some improved designs and applications. However, this accomplishment is not made without limitations. One of the limitations is that it is applicable only to a handful of geometries which were reported previously [5]. This is not really important since the basic properties, such as impedance, patterns, efficiency, and bandwidth, for various geometries are essentially the same. The second, and the most important, limitation is that the theory is useful only for relatively thin microstrip antennas, perhaps on the order of a few hundredths of wavelength, depending on the accuracy desired.

A fourth approach is the most rigorous one in which integral equations can be formulated by imposing the boundary conditions and the source condition. Unfortunately, the exact solution to these equations is practically impossible

to obtain, and even the approximate numerical solution is very involved. So far only some fundamental work has been performed and hopefully it will lead to a solution in the next phase. The advantage of this approach is that it will be applicable for any antenna thickness and will also be useful for the design of microstrip surface wave antennas. In this Section, we shall summarize the improved theory and leave the discussion of the fourth approach to a later section.

Rectangular Patch

First, consider the most commonly used rectangular microstrip antenna as shown in Fig. 2.1. The electric field under the patch (assumed to be in the xy-plane with dimensions a × b), has a z-component only and can be represented as

$$E_z = jk_0\eta_0 \sum_{m=0}^{\infty}\sum_{n=0}^{\infty} \frac{\phi_{mn}(x,y)\phi_{mn}(x',y')}{k^2 - k_{mn}^2} j_0\left(\frac{m\pi d}{2a}\right) \qquad (2.1)$$

where $k^2 = (1-j\delta_{eff})k_0^2$, $k_0 = 2\pi f/v$, f = frequency, v = speed of light, ε_r = relative dielectric constant = $\varepsilon_d/\varepsilon_0$, δ_{eff} = effective loss tangent = $1/Q$, $\eta_0 = 377\ \Omega$, $k_{mn}^2 = (m\pi/a)^2 + (n\pi/b)^2$, $j_0(x) = \sin(x)/x$, $\phi_{mn}(x,y) = \left[\frac{\varepsilon_{0m}\varepsilon_{0n}}{ab}\right]^{1/2}$ $\cos(m\pi x/a)\cos(n\pi y/b)$, $\varepsilon_{0m} = 1$ for $m = 0$ and 2 for $m \neq 0$, and d is the "effective width" of a uniform strip of z directed source current of one amp.

There is an alternative representation based on the modal-matching to a current source of one ampere. It contains only a single summation, and therefore is more suitable for numerical computation. This is shown below:

$$E_z = \sum_{m=0}^{\infty} \begin{Bmatrix} A_m \cos \beta_m(y-b) \\ B_m \cos \beta_m y \end{Bmatrix} \cos \frac{m\pi}{a}x \ , \text{ for } \begin{cases} y' \le y \le b \\ 0 \le y \le y \end{cases} \qquad (2.2)$$

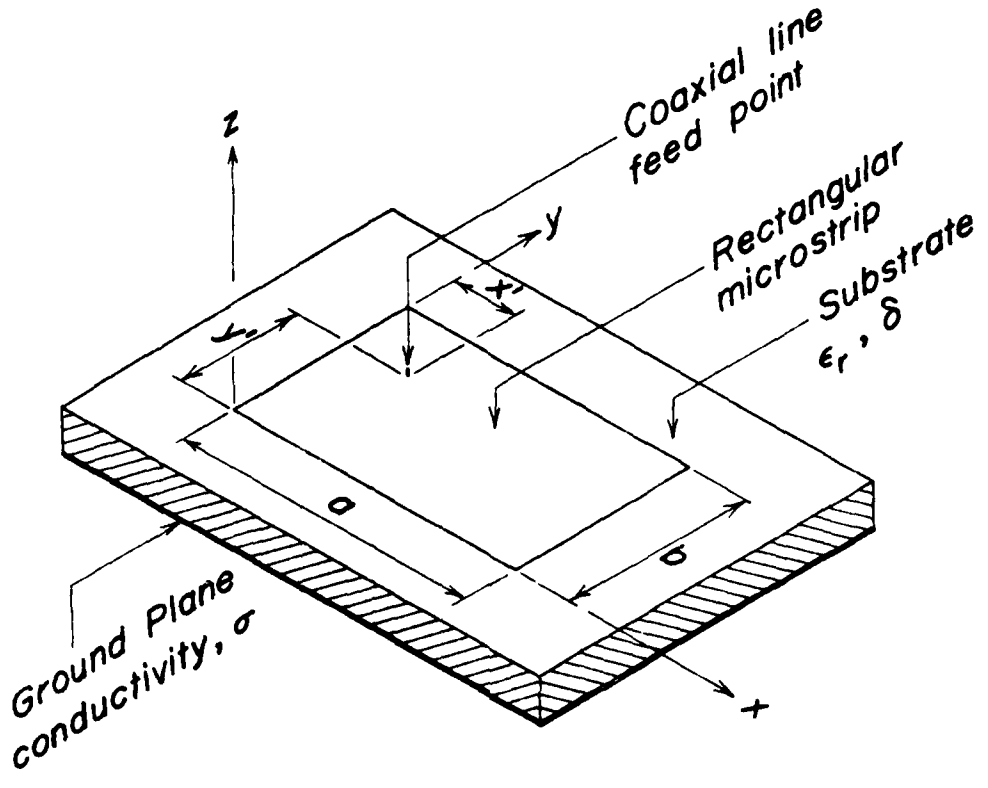

Figure 2.1. Geometry of a rectangular microstrip antenna.

where

$$A_0 = j\sqrt{\frac{\mu}{\varepsilon_d}}\ \frac{\cos ky'}{a \sin kb}$$

$$B_0 = j\sqrt{\frac{\mu}{\varepsilon_d}}\ \frac{\cos k(y' - b)}{a \sin kb}$$

$$A_m = \frac{j4\omega\mu}{m\pi}\ \frac{\cos m\pi d/2a}{\beta_m d \sin \beta_m b} \cos m\pi x'/a \cos \beta_m y'$$

$$B_m = \frac{j4\omega\mu}{m\pi}\ \frac{\cos m\pi d/2a}{\beta_m d \sin \beta_m b} \cos m\pi x'/a \cos \beta_m (y' - b)$$

$$\beta_m = \sqrt{k^2 - (m\pi/a)^2} \quad , \qquad m = 1,2,\ldots \quad .$$

Circular Patch

For a disk patch of radius "a" and fed with a uniform current source of one ampere at $\rho = \rho'$ and $|\phi| \leq \phi_W/2$, the electric field is given below:

$$E_z = \Sigma \begin{Bmatrix} A_m J_m(k\rho) + B_m Y_m(k\rho) \\ C_m J_m(k\rho) \end{Bmatrix} \cos m\phi\ \frac{\sin m\phi_W}{m\phi_W} \ , \text{ for } \begin{cases} \rho' \leq \rho \leq a \\ 0 \leq \rho \leq \rho' \end{cases} \tag{2.3}$$

where

$$A_m = \frac{-j\omega\mu\ Y_m'(ka)\ J_m(k\rho')}{2(1 + \delta_{m0})\ J_m'(ka)}$$

$$B_m = \frac{j\omega\mu\ J_m(k\rho')}{2(1 + \delta_{m0})}$$

$$C_m = -\frac{2\omega\mu[J_m(k\rho')\ Y_m'(ka) - Y_m(k\rho')\ J_m'(ka)]}{2(1 + \delta_{m0})\ J_m'(ka)}$$

$$\delta_{m0} = \begin{cases} 1 \ , & m = 0 \ , \\ 0 \ , & m \neq 0 \ . \end{cases}$$

Radiated Power Computation

Applying Huygen's principle to the outer surface of the cavity and neglecting the electric current flowing on the outer surface of the microstrip antenna one obtains on the magnetic wall C the Huygen's magnetic current source

$$\vec{K} = 2\hat{n} \times \hat{z}E_z \quad ,$$

where $\hat{n}$ is the outward normal to the H-wall, and the factor of 2 accounts for the presence of the ground plane. The electric vector potential of K is

$$\vec{F}(\vec{r}) = \varepsilon_0 \int_C \frac{\vec{K}(\vec{r}')}{4\pi|\vec{r} - \vec{r}'|} e^{-jk_0|\vec{r}-\vec{r}'|} \, dl(\vec{r}) \quad , \tag{2.4}$$

and the far field at $\vec{r}$ is

$$E_\theta = \eta H_\phi = jk_0 F_\phi = jk_0(-F_x \sin\phi + F_y \cos\phi)$$

$$E_\phi = -\eta H_\theta = -jk_0 F_\theta = -jk_0(F_x \cos\theta \cos\phi + F_y \cos\theta \sin\phi) \quad . \tag{2.5}$$

The total radiated power is

$$P_r = \mathrm{Re} \int_0^{\pi/2} \int_0^{2\pi} (E_\theta H_\phi^* - E_\phi H_\theta^*) r^2 \sin\theta \, d\phi \, d\theta \quad . \tag{2.6}$$

Computation of Power Losses and Stored Energies

The time-averaged stored electric energy is given by

$$W_e = \frac{t\varepsilon_d}{2} \int_S |E|^2 \, dS \tag{2.7}$$

where t is the thickness, ε_d the permittivity of the substrate, S the patch surface area, and E is given by Eqs. (2.2) and (2.3) for rectangular and circular patch respectively. At resonance the time-averaged stored magnetic energy W_h equals W_e.

The loss in the dielectric with loss tangent δ is

$$P_d = \omega\varepsilon_d\delta t \int_S |E|^2 \, dS = 2\omega\delta \, W_e \tag{2.8}$$

The loss in the copper-cladding with conductivity σ is approximately

$$P_{cu} = \frac{4}{\sigma\Delta t\mu} W_h = \frac{4}{\sigma\Delta t\mu} W_e \tag{2.9}$$

near resonance, where $\Delta = [2/\omega\mu\sigma]^{1/2}$ is the skin depth, and the factor 2 accounts for the surface area at $z = 0$ and t.

Input Impedance Computation

Define the driving voltage at the feed as

$$V = tE \text{ (at the feed, averaged over the feed width)} \quad . \tag{2.10}$$

Then the antenna input impedance can be computed from any one of the following three formulas:

$$Z = [V/(-I)] \text{ at the feed} \tag{2.11}$$

$$Z = [P + j2\omega(W_h - W_e)]/|I|^2 \tag{2.12}$$

$$Z = |V|^2/[P + j2\omega(W_e - W_h)] \quad , \tag{2.13}$$

where $P = P_r + P_d + P_{cu}$. It shall be noted that Eqs. (2.1) - (2.3) are derived for $I = 1$ amp. Obviously, it is simpler to use the first formula (2.11) for computing Z. Details for various cases can be found in the Interim Reports [6,7].

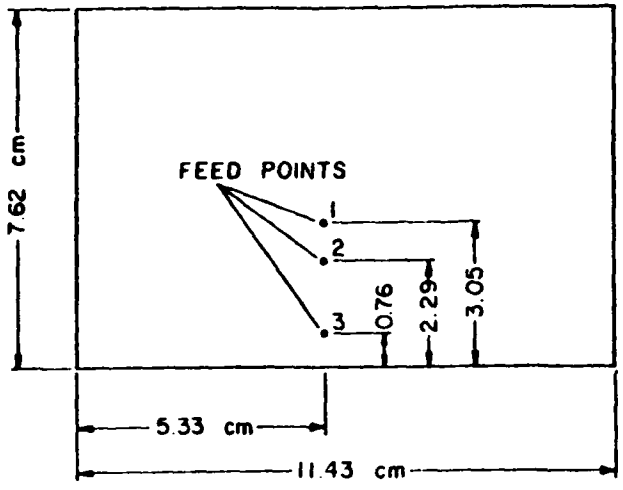

RECTANGULAR MICROSTRIP ANTENNA

SUBSTRATE REXOLITE 2200
1/16" NOMINAL THICKNESS

(a)

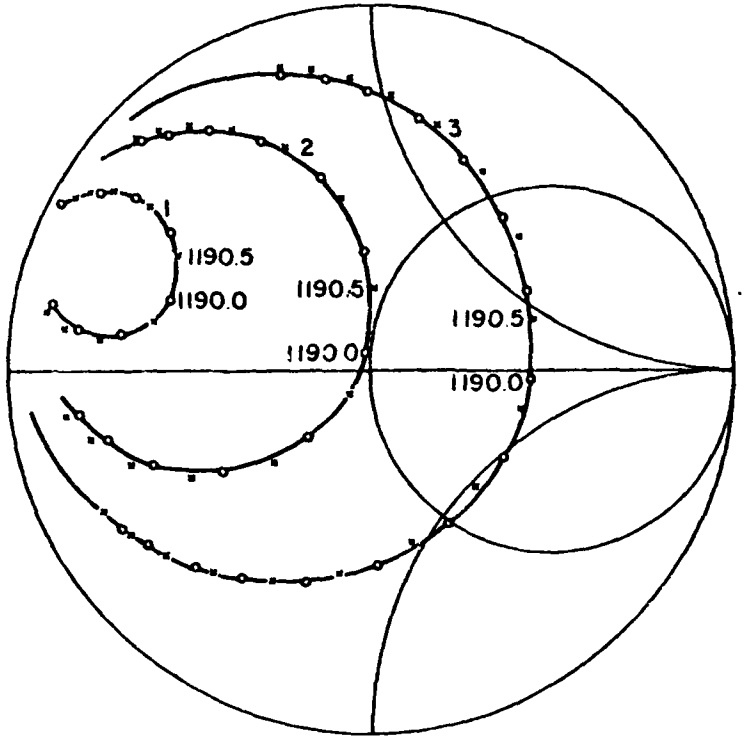

MEASURED LOCUS

× × COMPUTED LOCUS

INCREMENT 5 MHz

(INCREASING FREQUENCY IS CLOCKWISE)

(b)

Figure 2.2. (a) Dimensions and feed locations of rectangular microstrip antenna.
(b) Measured and computed impedance loci.

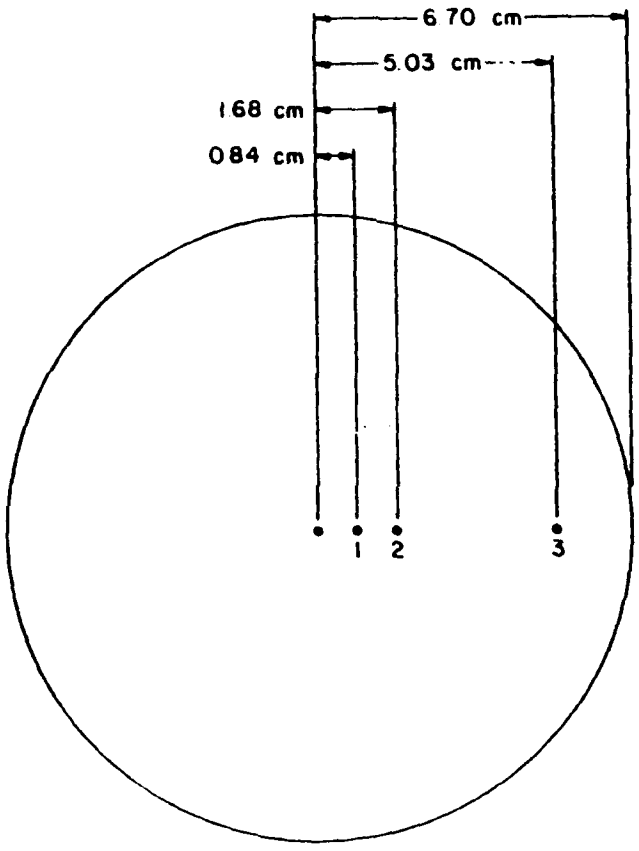

DISK MICROSTRIP ANTENNA

SUBSTRATE REXOLITE 2200
1/16" NOMINAL THICKNESS

(a)

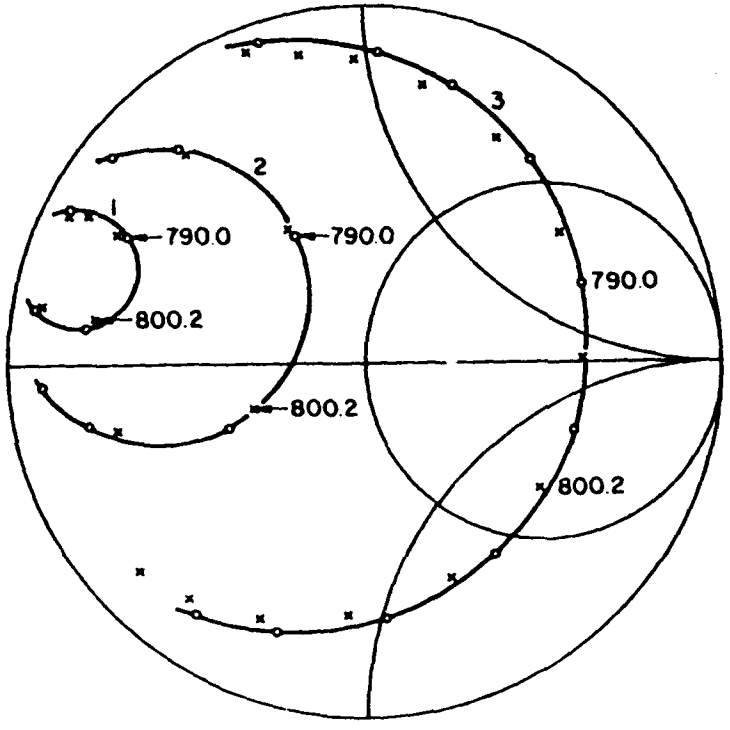

MEASURED LOCUS

COMPUTED LOCUS

INCREMENT: 5 MHz

(INCREASING FREQUENCY IS CLOCKWISE)

(b)

Figure 2.3. (a) Dimensions and feed locations of circular disk microstrip antenna.
(b) Measured and computed impedance loci.

Verification of the Theory

Two typical results, one for rectangular and the other for circular microstrip antenna, are shown in Figs. 2.2 and 2.3. It is seen that the theoretically predicted impedance characteristics agree with those measured remarkably well at every frequency considered.

Efficiency Analysis

Figs. 2.4 and 2.5 show the dependence of various power losses, including the radiated power, on the width "a" of a rectangular patch antenna and on the substrate thickness "t," respectively, when the (0,1) mode is excited. It is interesting to see firstly that the antenna efficiency increases with "a" but more slowly after a certain value, and secondly, that the efficiency increases sharply with t at the beginning, but may even decrease for large t due to a significant portion of the power being converted into surface wave. Thus very thin microstrip antenna is not efficient.

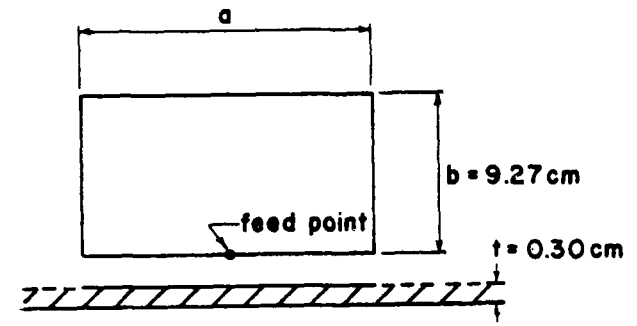

Frequency: 1 GHz
Copper: σ = 100 KΩ/cm
Substrate: δ = 0.001
ϵ_r = 2.62

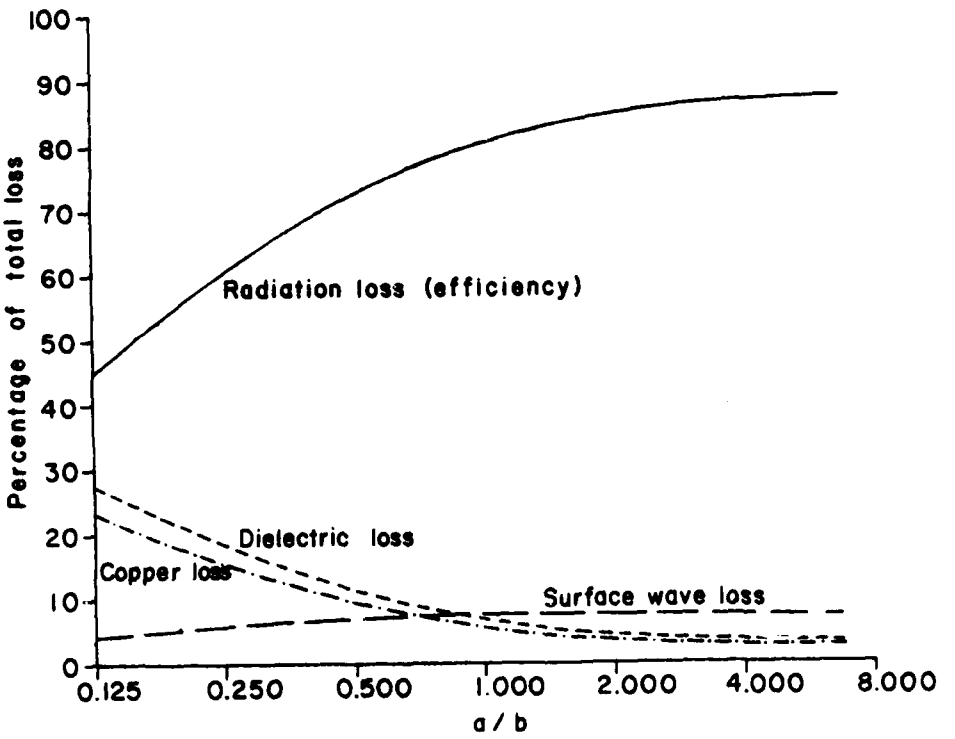

Figure 2.4. Computed various power losses vs. the aspect ratio a/b of a rectangular microstrip antenna.

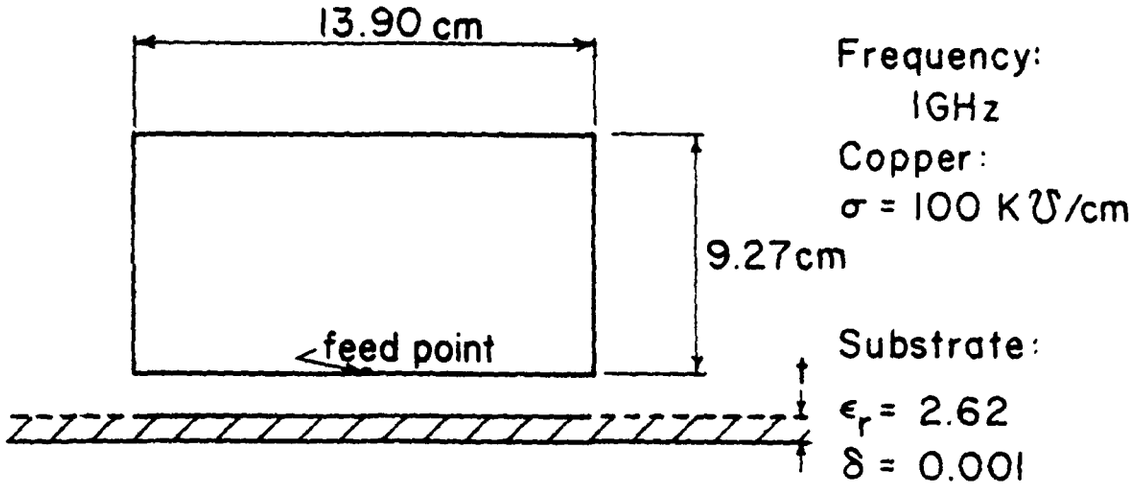

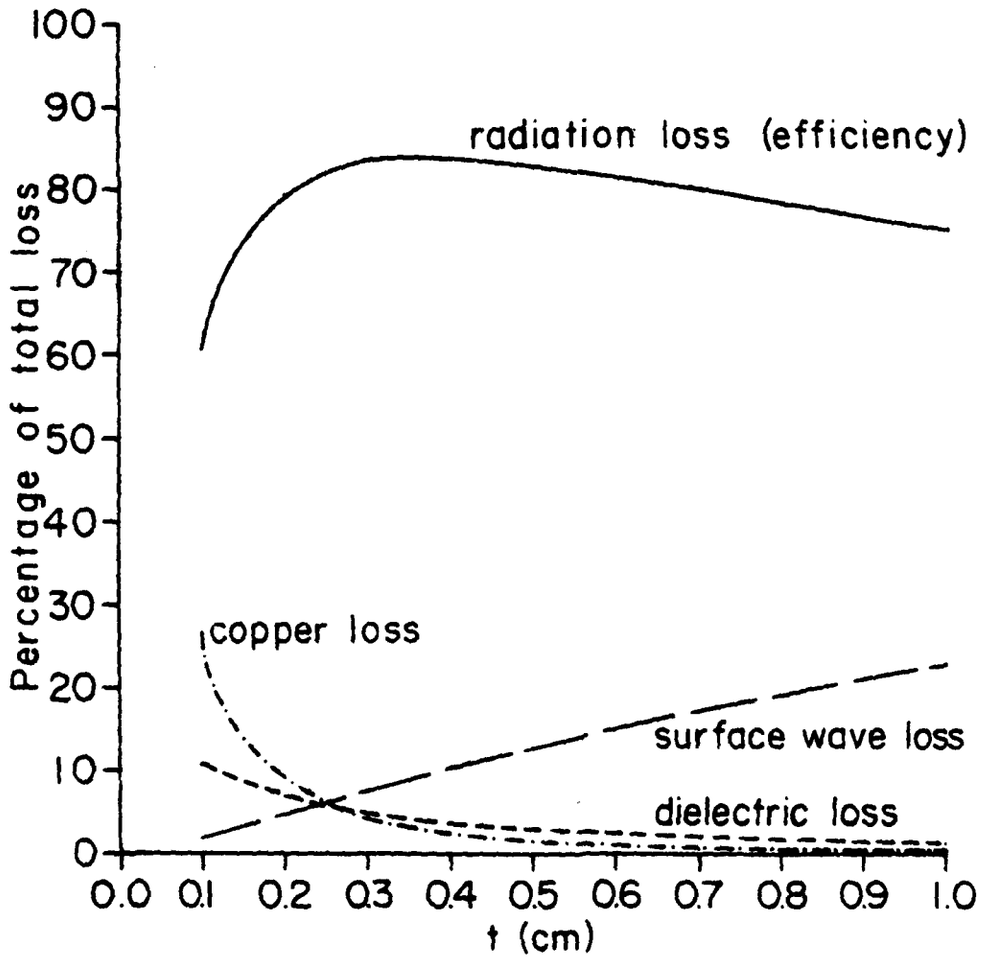

Figure 2.5. Computed various power losses vs. thickness t of a rectangular microstrip antenna made of Rexolite.

III. Circularly Polarized Microstrip Antennas

It is well-known that circular polarization can be produced by a microstrip antenna with a single input port and no phasing network. But all works reported are based on a trial-and-error approach either experimentally [8] or with a computer [9]. Both of these approaches are not only time-consuming and costly, but also provide little physical insights into the mechanism of operation. In this study the conditions for generating circular polarization are formulated and some surprisingly simple but very accurate design formulas are derived. Briefly, the condtions are:

(a) The microstrip antenna must be capable of supporting two degenerated modes; i.e., two modes having the same resonant frequency;

(b) the two modes must radiate two orthogonal field components in the direction normal to the patch;

(c) a proper perturbation of the patch geometry can be made such that the degenerated wave number will split into two, say k_1 and k_2, with their difference $|k_1 - k_2|$ to the operating wave number k ratio equal to the inverse of the Q-factor of the patch; i.e.,

$$|k_1 - k_2|/k = 1/Q \tag{3.1}$$

(d) the feed must be placed at an appropriate location for the desired polarization.

For simple geometries, such as squares and circles, the above equation can be translated into the required geometrical perturbation. There are different ways to accomplish this, but in the following the energy perturbation method will be presented because of its simplicity.

Perturbation Theory

Assume that a magnetic cavity of volume v and resonant wave number k_0 is perturbed by removing (or adding) a small volume ΔV. Then the change in resonant wave number from k_0 to k_1 is given by

$$\frac{k_1 - k_0}{k_0} = \frac{\Delta W_e - \Delta W_h}{W_e + W_h} = \frac{\int_{\Delta v}(\varepsilon|E|^2 - \mu|H|^2)\, dv}{\int_v(\varepsilon|E|^2 + \mu|H|^2)\, dv} \quad . \tag{3.2}$$

where W_e and W_h are time-averaged stored electric and magnetic energy in v , respectively, ΔW_e and ΔW_h are those in perturbed volume Δv, and ε and μ are, respectively, the permittivity and permeability of the medium in the cavity.

Nearly Square Patch

For a rectangular patch defined by $|x| \leq a/z$ and $|y| \leq b/2$ with $0 < a - b = c << a$,

$$E_z = \sin(\pi y/b)$$

$$H_x = (j\pi/\omega\mu b)\cos(\pi y/b) \quad .$$

Then,

$$\Delta W_e = \varepsilon a\int_{b/2}^{a/2} \sin^2(\pi y/b)\, dy = \varepsilon ac/2$$

$$\Delta W_h = \mu a\int_{b/2}^{a/2} (\pi/\omega\mu b)^2 \cos^2(\pi y/b)\, dy \approx 0$$

$$W_e = (\varepsilon a/2)\int_{-a/2}^{a/2} \sin^2(\pi y/2)\, dy = \varepsilon a^2/4$$

Since at resonance, $W_h = W_e$, one obtains

$$\frac{k_{rect} - k_{square}}{k_{square}} = \frac{\Delta W_e - \Delta W_h}{2W_e} = \frac{c}{a} = \frac{1}{Q} \tag{3.3}$$

This implies the required dimension of nearly square patch for CP is as follows:

$$a/b = 1 + (1/Q) \quad . \tag{3.4}$$

This result agrees exactly with that obtained in [6] through a different approach. The surprisingly high accuracy of this formula has been verified experimentally as reported in [6].

Nearly Circular Disk Patch

Let the semi-major and semi-minor axes of an ellipse be a and b respectively, and $a - b = c << a$. Then

$$(x/a)^2 + (y/b)^2 = 1 \quad .$$

In terms of polar coordinates (ρ,ϕ,z), the ellipse can be expressed approximately as

$$\rho = [1 - (c/b)\ sin^2\phi]\ a + O(c^2/a^2) \quad . \tag{3.5}$$

Now consider first a circular patch of radius a, excited for the dominant mode (1,1). The fields are

$$E_z = J_1(k_{11}\rho)\ \cos\phi$$

$$H_\phi = -(jk/\omega\mu)\ J_1'(k_{11}\rho)\ \cos\phi$$

$$H_\rho = -(jk/\omega\mu)\ J_1(k_{11}\rho)\ \sin\phi$$

where the modal wave number k_{11} satisfies the characteristic equation

$$J_1'(k_{11}a) = 0 \quad , \quad \text{and} \quad k_{11}a = 1.841 \quad . \tag{3.6}$$

The change in stored electric energy from a circular patch to an elliptical patch is approximately

$$\Delta W_e = (\varepsilon/2) \int_0^{2\pi} \int_{a-(ac/b)\sin^2\phi}^{a} J_1^2(k_{11}\rho)\rho d\rho \cos^2\phi d\phi$$

$$\approx (\varepsilon\pi a^2 c/b)\, J_1^2(k_{11}a) \quad . \tag{3.7}$$

Similarly, the change in stored magnetic energy is

$$\Delta W_h \approx (3\pi c/8\omega^2\mu b)\, J_1^2(k_{11}a) \quad .$$

The total stored electric energy is

$$W_e = (\varepsilon/2) \int_0^{2\pi}\int_0^{a} J_1^2(k_{11}\rho) \cos^2\phi\, \rho d\rho\, d\phi$$

$$= (\varepsilon\pi\rho^2/4)\{J_1'(k_{11}\rho) + [1 - (k_{11}\rho)^{-2}]\, J_1^2(k_{11}\rho)\}\Big|_{\rho=0}^{a}$$

$$= (\varepsilon\pi a^2/4)[1 - (k_{11}a)^{-2}]\, J_1^2(k_{11}a) \quad .$$

Thus when the antenna is fed at x = a (or -a) and y = 0, the (1,1) mode will be excited, and the difference between the resonant wave number k_{e1} of the elliptical patch and k_a of the circular patch of radius a is given by

$$\frac{k_{e1} - k_a}{k_a} = \frac{\Delta W_e - \Delta W_h}{2W_e} \approx (c/4a)\, \frac{1 - 3(k_{11}a)^{-2}}{1 - (k_{11}a)^{-2}} \approx 0.0408\ (c/a) \quad . \tag{3.8}$$

When the antenna is fed at x = 0 and y = b (or -b), the modal field $E_z = J_1(k_{11}\rho)\sin\phi$ will be excited. For this mode, one can either repeat the above computation, or simply interchange a with b and the integration limits in Eq. (3.7) to "from b to b+ (bc/a) $\sin^2\phi$." The difference between resonant wave number k_{e2} of the elliptical patch and k_b of a circular path of radius b is then given by

$$\frac{k_{e2} - k_b}{k_b} = -0.0408(c/a) \tag{3.9}$$

From Eqs. (3.1), (3.8), and (3.9), one obtains

$$\frac{1}{Q} = \frac{k_{e2} - k_{e1}}{k_a} = -0.0816(c/a) + \frac{k_b - k_a}{k_a}$$

$$= -0.0816(c/a) + \frac{a - b}{a}$$

$$= 0.9184(c/a) \quad . \tag{3.10}$$

Hence, the required dimensions or axial ratio of the elliptical patch is given by

$$c/a = 1.0887/Q$$

or

$$a/b = 1 + (1.0887/Q) \tag{3.11}$$

Similar to a nearly square microstrip antenna, when a feed is placed along the line $\phi = 90°$ (or $-90°$), LHCP (or RHCP) wave will be radiated along the z-axis.

Long [9] has made measurements at around 1.3 GHz for two CP elliptical patch antennas with thickness $t_1 = 0.16$ cm and $t_2 = 0.32$ cm, respectively, and both having $a = 4.00$ cm. The "best" ratio (b/a) for CP operation among several trials by him is listed in Table 1. Also listed are the values predicted by Shen [9] who used a computer to search for the "best" frequency of operation for a given small axial ratio.

Table 1. Comparison of Measured and Predicted Values of b/a of Elliptical Patch for CP

	Measured Q due to Long [10]	(b/a)		
		Exp (by Long)	Computed (by Shen)	Computed [by Eq. (3.11)]
t_1 = 0.16 cm	96.35	0.984	0.989	0.989
t_2 = 0.32 cm	46.35	0.976	0.979	0.976

The values in the last column are computed using Long's measured Q which can also be computed readily from the losses and the radiated power of the circular patch as discussed in Section 2, or Ref. [7]. The radiation pattern and impedance characteristics of the CP elliptical patch antenna are very similar to those of the circular patch except for a sharp cusp in the impedance locus. Therefore, there is no need to use the complicated Mathieu functions, nor their approximate expressions. It should be noted that the perturbation method, although yields results almost in perfect agreement with the measured for both cases discussed above, yet failed to predict the required dimensions accurately for a square patch with two opposite corners removed [11]. Apparently, in that case new edge conditions and therefore new fringing field are created as the corners are removed. Therefore, this investigation suggests that the perturbation method is applicable whenever the edge condition is not altered drastically

Polarization Tuning

In the antennas discussed above, a certain polarization can be obtained only with the feed placed at an appropriate location in the patch, and therefore in order to change the polarization the feed must be moved accordingly. To

alleviate this inconvenience the variation of polarization can also be achieved for a fixed feed by varying the DC biases of two capacitance diodes loaded at adjacent sides of a nearly square patch [11]. If the diodes are connected at the nulls of the (0,1) and (1,0) modes, then their effect on the tuning will be approximately independent of each other. An experimental sample antenna has been fabricated as shown in the sketch in Figs. 3.1, in which two low pass filter circuits for each diode are also shown. Fig. 3.2 shows the measured patterns for the LHCP and the RHCP fields at 840 GHz.

The tuning can also be accomplished by placing switching diodes properly located in the patch. Obviously, this technique is practical only for very few tuning steps. This will be discussed in Section IV.

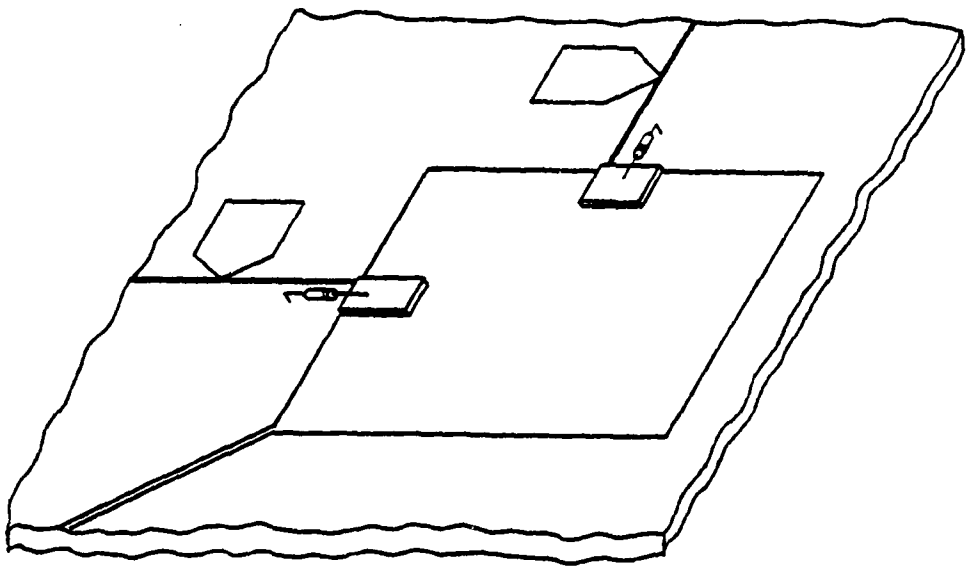

Figure 3.1a. Double-tuned microstrip antenna for various polarizations.

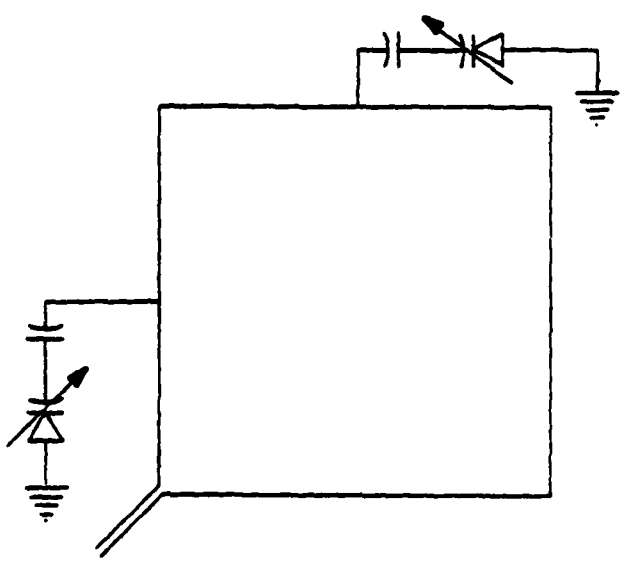

Figure 3.1b. Double-tuned microstrip antenna schematic.

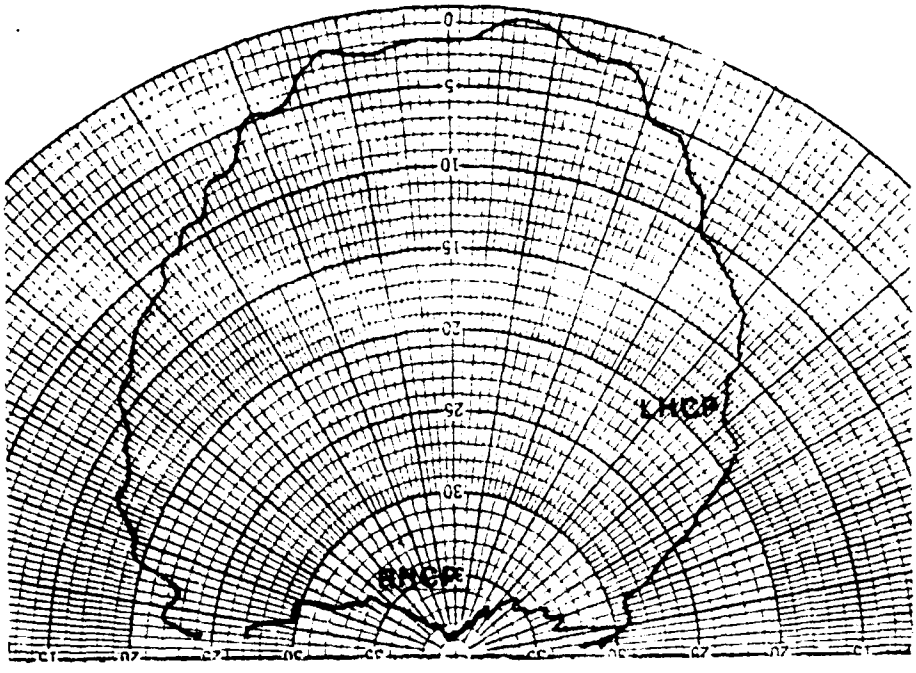

Figure 3.2a. Left and right hand CP patterns of the double-tuned microstrip antenna biased for LHCP.

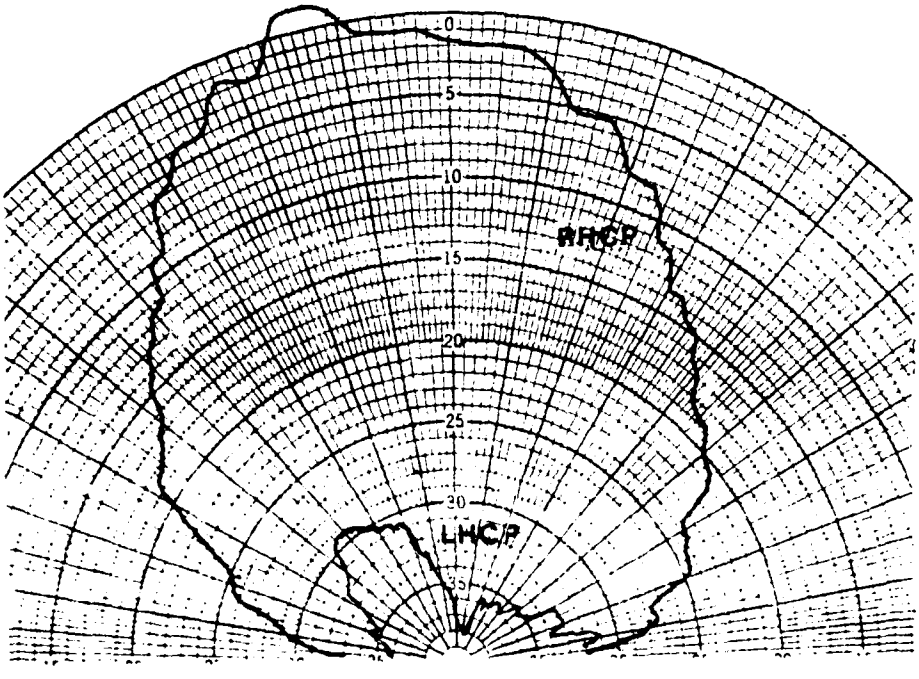

Figure 3.2b. Left and rifht hand CP patterns of the double-tuned microstrip antenna biased for RHCP.

IV. WIDE-BAND MULTIPORT THEORY

Schaubert, Farrar, Sindoris, and Hayes [15] have shown that by loading other ports of a multiport microstrip antenna, the apparent resonant frequency can be shifted considerably away from that of any of the resonant frequencies of its unloaded counterpart. Thus, in any modal expansion of the field, no particular resonant mode will dominate at some operating frequencies in contrast to the case of the unloaded antenna. Indeed, Schaubert, et. al. have given experimental data indicating that by properly loading a microstrip antenna the operating frequency of the radiator can be changed anywhere in a range containing three different resonant frequencies of the corresponding unloaded antenna. Thus, a multiport theory which is suited to such wide ranges of frequencies is needed to adquately predict the behavior of loaded antennas. Such a theory is proposed in this summary.

This wide-band theory is a modification of approach [6]. The "Z-parameters" of a multiport lossy cavity which models the antenna can be expressed as a sum over the resonant modes of the cavity:

$$Z_{pq} = -jk_0\eta_0 t \sum_{m=0}^{\infty} \sum_{n=0}^{\infty} T_{mn}^{pq}/(k^2 - k_{mn}^2) \quad , \qquad (4.1)$$

where

$$k_{mn}^2 = \left(\frac{m\pi}{a}\right)^2 + \left(\frac{n\pi}{b}\right)^2 \quad ,$$

$$T_{mn}^{pq} = \phi_{mn}(x_p,y_p)\ \phi_{mn}(x_q,y_q)\ j_0^2(m\pi d/2a) \quad ,$$

$$j_0(x) = \sin(x)/x \quad ,$$

$$\phi_{mn} = (\varepsilon_{om}\varepsilon_{on}/ab)^{1/2} \cos(m\pi x/a) \cos(n\pi y/b) \quad ,$$

$$\varepsilon_{om} = 2 \text{ for } m = 0 \text{ and } 1 \text{ otherwise} \quad ,$$

$\eta_0 = 377\Omega$, k_0 is the free space wave number, a, b, and t are the patch dimensions and dielectric thickness, respectively, and (x_s, y_s) are the coordinates of the $s^{\underline{th}}$ port.

In this summation, the parameter "d" is the "effective feed width" which is used to model the feed (and probe to which any load may be connected in the other ports). The current that flows in the feed is assumed to be a uniform thin band of width d of current flowing from the ground plane to the patch. This parameter has been empirically determined and it appears to be on the order of five times the probe diameter. According to the theory reported in [6], the wave number within the cavity, k, is set equal to

$$k = \varepsilon_r k_0 \left(1 - j \frac{1}{Q}\right)^{1/2}$$

where ε_r is the refractive index of the dielectric, and Q is the quality factor of the antenna which can be computed accurately from the formula,

$$Q_{mn} = 1/(1/Q_{mn}^{rad} + \delta + \Delta/t) \quad ,$$

where

$$\delta = \text{dielectric loss tangent} \quad ,$$

$$\Delta = \text{skin depth in cladding,}$$

$$Q_{mn}^{rad} = \frac{\pi^2 k_0 a k_0 b}{\varepsilon_{om} \varepsilon_{on} k_0 t} \frac{1}{\alpha_{mn}} \cdot r^2 \quad ,$$

$$\alpha_{mn} = \int_0^{\pi/2} \int_0^{2\pi} \sin\theta \, d\theta \, d\phi \, |\vec{F}|^2 \quad ,$$

$$F_\theta = -F_x \sin\phi + F_y \cos\phi$$

$$F_\phi = (F_x \cos\phi + F_y \sin\phi) \cos\theta \quad ,$$

$$F_x = g \frac{(k_0 a)^2 \sin\theta\cos\phi}{(k_0 a \sin\theta\cos\phi)^2 - (m\pi)^2} \quad ,$$

$$F_y = g \frac{(k_o b)^2 \sin\theta\sin\phi}{(k_0 b\sin\theta\sin\phi)^2 - (n\pi)^2}$$

for the (m,n) mode of interest. In the limited band theory, reported in [6], the inner sum of (4.1) was summed "in closed form" leading a one-dimensional series whose convergence was further accelerated by a Kummer's transformation. That procedure works well as long as the frequency band of interest is about the (m,n)th resonant frequency. In the present theory, however, the wave number k in <u>each</u> term of the series in (4.1) is replaced by its own particular

$$k'_{mn} = \epsilon_r k_0 (1 - j \frac{1}{Q_{mn}})^{1/2}$$

up to a certain limiting wave number. This limiting wave number, k_2, is twice the wave number, $k_1 = \epsilon_r 2\pi f_0/c$, where f_0 is the maximum frequency at which the antenna is to be analyzed and c is the speed of light.

Terms of (4.1) with $k_{mn} < k_2$, are summed directly. The remaining terms of the series are summed as follows. For $k_{mn} \geq k_2 = 2k_1 > 2k = 2\epsilon_r k_0$,

$$\frac{1}{k^2 - k_{mn}^2} = \frac{1}{k_{mn}^2}[0.989 + 1.331 \frac{k^2}{k_{mn}^2} + e(k/k_{mn})] \ , \ |e(x)| < 0.013.$$

Therefore, the contribution to the infinite series in (4.1) due to m and n such that $k_{mn} \geq k_2$, can be adequately approximated by

$$0.989(T_0 - S_0) + 1.331 \ (T_1 - S_1)k^2 \quad ,$$

where

$$T_\ell = \sum_{k_{mn}<k_2}{}' T_{mn}^{pq}/k_{mn}^{2\ell+2} \quad ,$$

$$S_\ell = \sum_{m=0}^{\infty} \sum_{n=0}^{\infty}{}' T_{mn}^{pq}/k_{mn}^{2\ell+2} \quad , \qquad \ell = 0,1 \ ;$$

where ' means excluding the point (m,n) = (0,0) from sum. Then the inner series defining S_0 and S_1 are summed in "closed form" and the resulting one-dimensional sums are evaluated by some simple approximate formulas. The T's and S's above are constants dependent only on the geometrical and material parameters of the antenna. Thus,

$$Z_{pq} = -jk_0\eta_0 \left[\sum_{k_{mn}<k_2}' \frac{T_{mn}^{pq}}{(k'_{mn})^2 - k_{mn}^2} + a_0 + a_1 k^2 \right]$$

$$a_0 = 0.989(T_0 - S_0) \quad , \quad a_1 = 1.331\ (T_1 - S_1).$$

This single expression is valid around every resonant frequency between D.C. and f_0.

With the Z parameters thus computed, the driving point impedance of a loaded multiport microstrip antenna can be evaluated using the known load impedance matrix by the usual network analysis. Schaubert, et. al [15] have made an investigation of a rectangular patch with a = 9.00 cm, b = 6.20 cm, ε_r = 2.55, and t = 0.16 cm. The antenna is fed with a cable at x' = 0, y' = 1.5 cm and a shorting stub is placed at x = a/2 and y = (b/2) - ℓ as shown in Fig. 4.1. They experimentally determined the operating frequency, defined as one at which the SWR is minimum for each of the stub positions ℓ (normalized with respect to b/2) as shown in Fig. 4.2. Also shown is the SWR vs. stub position. Using the theory and algorithm developed above, the operating frequencies for various stub positions can be predicted as shown in Fig. 4.3. Comparing this with that in Fig. 4.2, one will find an excellent agreement except for (1) a small shift, about 0.847%, in the frequency axis, and (2) a small discrepancy near d = b/2. It is believed that they are caused by the complicated fringing effect around

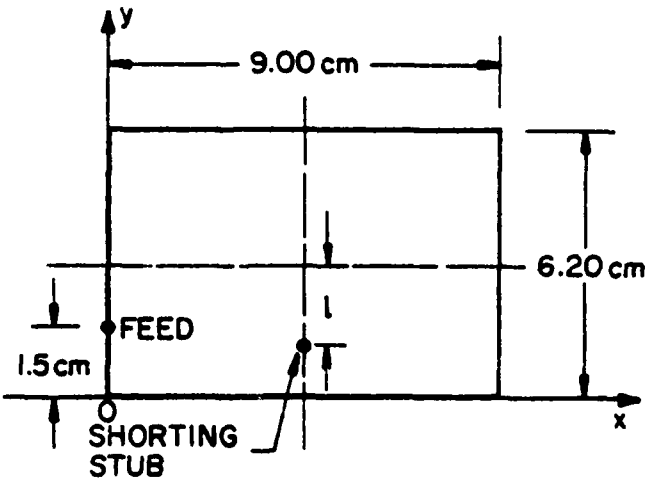

Figure 4.1. Geometry of a rectangular microstrip antenna with a tuning stub.

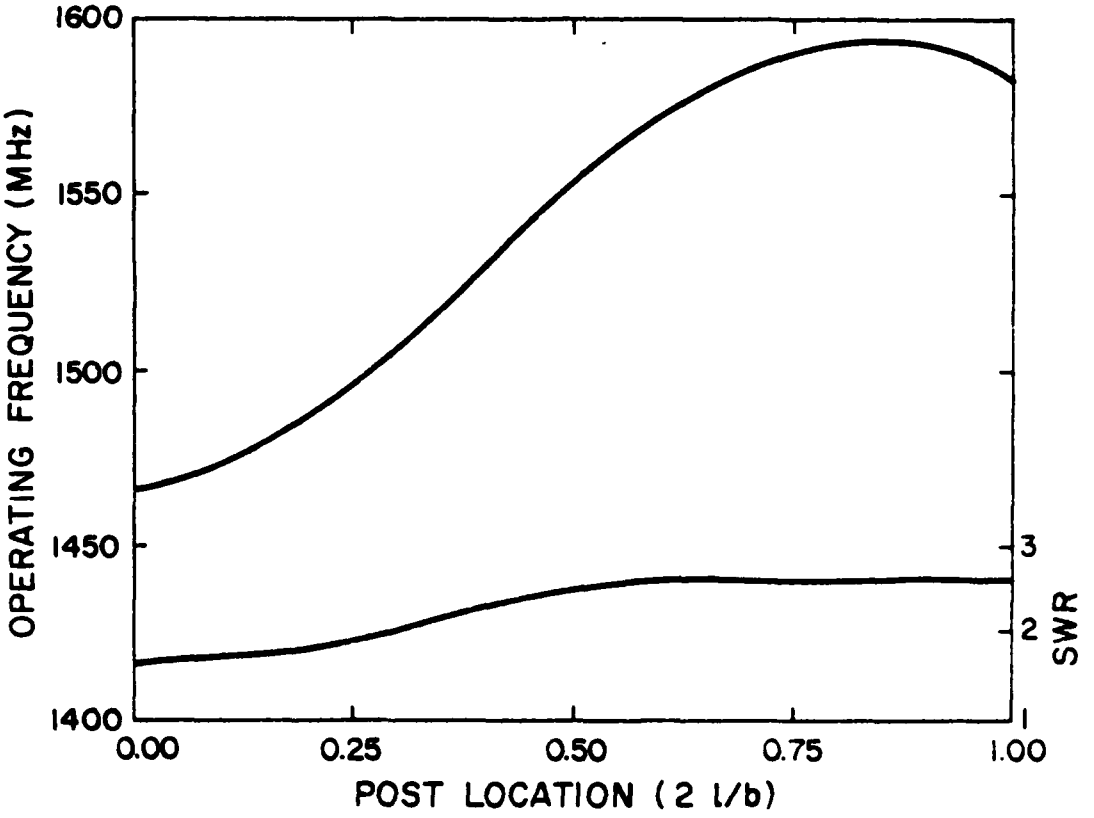

Figure 4.2. Plot of measured operating frequency vs. post position.

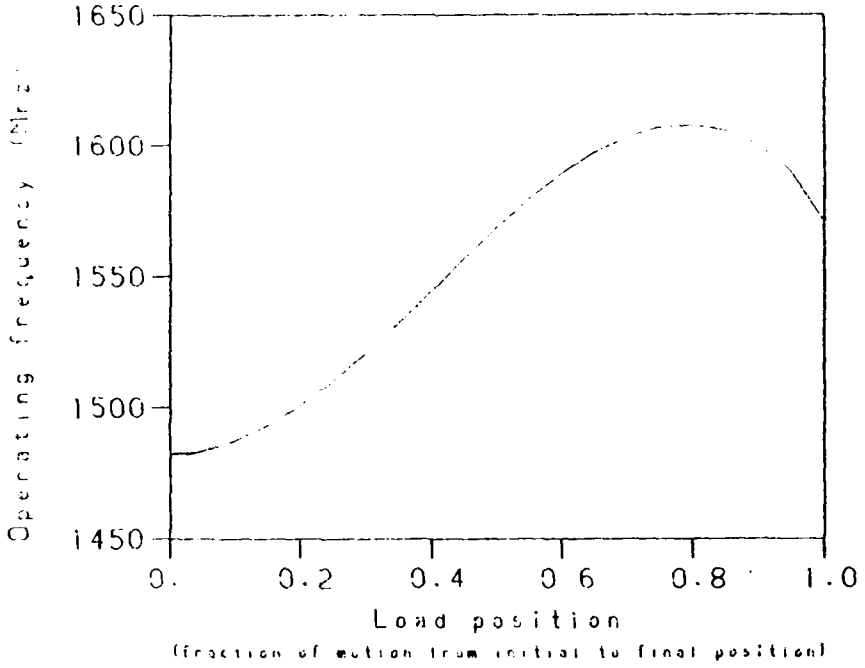

Dielectric = 2.55
Loss tangent = 0.0018
Conductivity = 428 KMhos/cm
Thickness = 0.16 cm
Feed width = 0.25 cm

Feed : (0.13, 1.50)
Load : (4.50, 3.10) ⟶ (4.50, 0.)

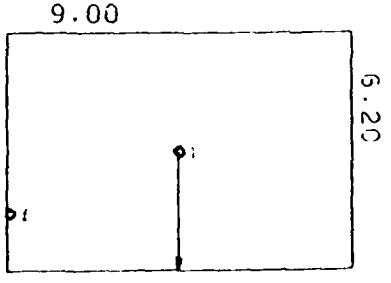

Figure 4.3. Theoretically predicted operating frequency vs. post position.

the feed and the shorting stub when they are near the edge of the patch. They could be accounted for by using appropriate values for the effective width.

Fig. 4.4 shows the measured and computed impedance loci for a square patch for CP operation. The agreement is nearly perfect. It may be noted that in this case both the feed and shorting stub are inside the patch.

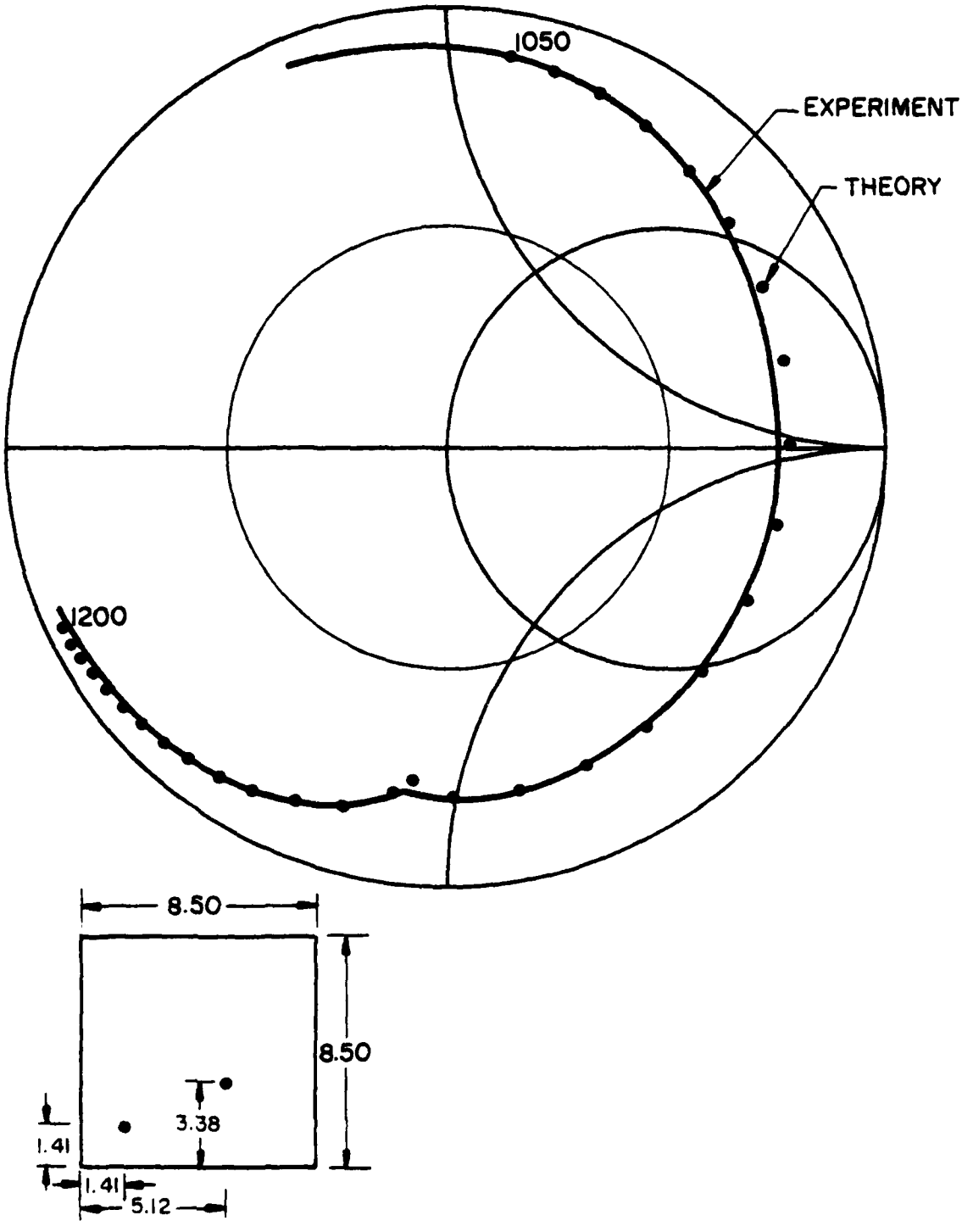

Figure 4.4. Comparison of theoretical and measured impedance loci of a loaded square microstrip antenna for CP operation. The feed is at (1.41, 1.41) and the shorting post at (5.12,3.38), all in centimeters.

V. ANNULUS AND QUADRULUS MICROSTRIP ANTENNAS

Most, if not all, microstrip antennas investigated extensively are characterized in geometry by that the patch is a simply connected region. In other words, the patch is bounded by a single closed curve. Since it is generally understood that it is the equivalent magnetic current along the boundary curve that radiates, one may speculate whether a patch bounded by two or more closed curves would have fundamentally different radiation patterns. To obtain a quick answer to this question, patches of two simple geometries are investigated; namely, an annulus and a "window" shaped rectangle (i.e., a rectangle with a concentric rectangular region removed. For convenience, it will be called "quadrulus"). The former can be studied analytically [5] while for the latter only numerical method is possible. As will be seen later from the measured results, their impedance loci and radiation patterns are not basically different from those of the patches of simply connected regions. Therefore, it seems that a major effort for the theoretical analysis of these antennas at this moment is not justified.

Figs. 5.1-5.3 show the measured impedance locus and radiation patterns of a circular disk patch antenna with radius equal to 6.75 cm and fed at the edge of the disk. They should be compared with the corresponding characteristics shown in Figs. 5.4 - 5.6 for an annulus patch of radii 6.63 cm and 1.77 cm, also fed at the edge of the outer circle.

Fig. 5.7 shows the geometry of the rectangular patch antenna and the "quadrulus" patch antenna investigated. The impedance loci and patterns for several lowest order modes of both patches are shown in Figs. 5.8-5.17. It should be noted that the power level was not maintained constant through the

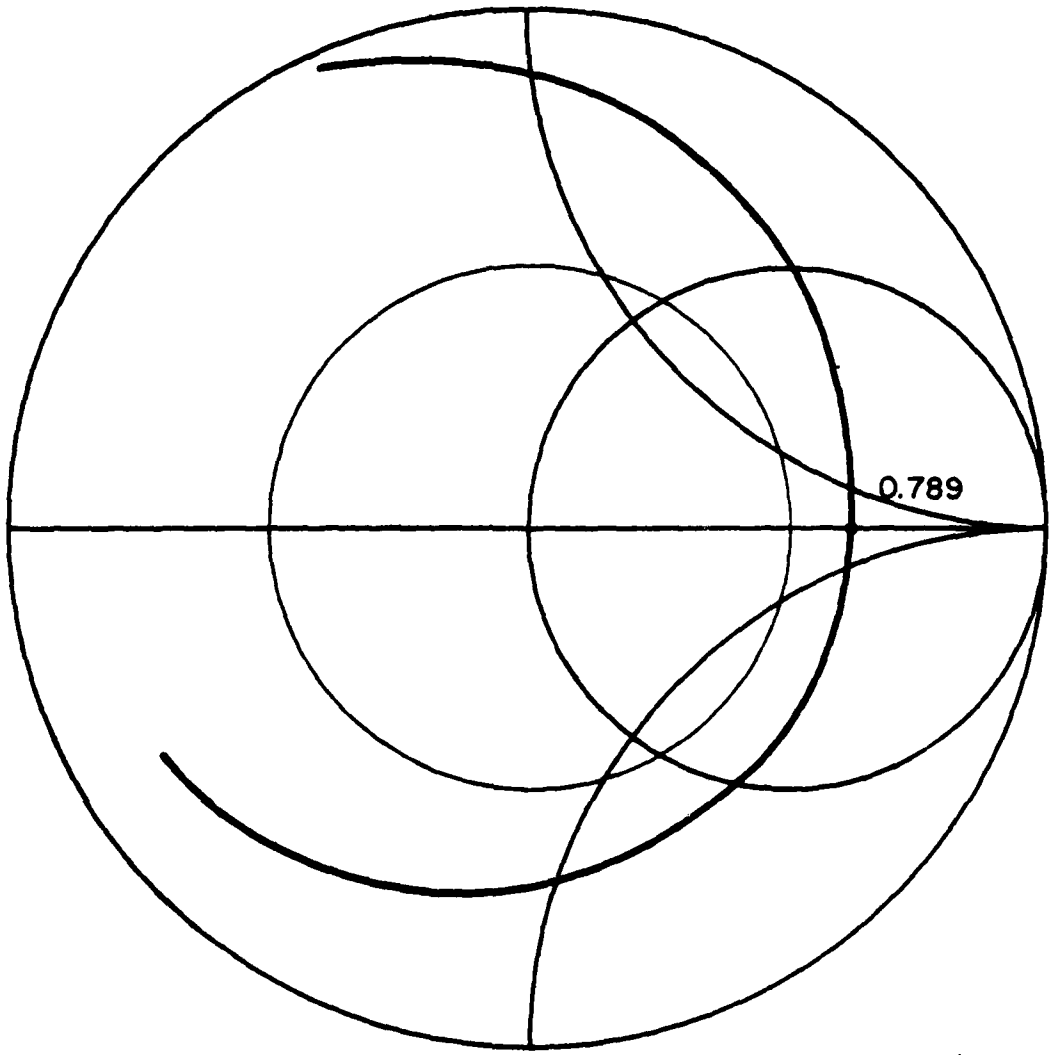

Figure 5.1 Impedance locus of a circular disk microstrip antenna of radius 6.75 cm, fed at the edge of the disk.

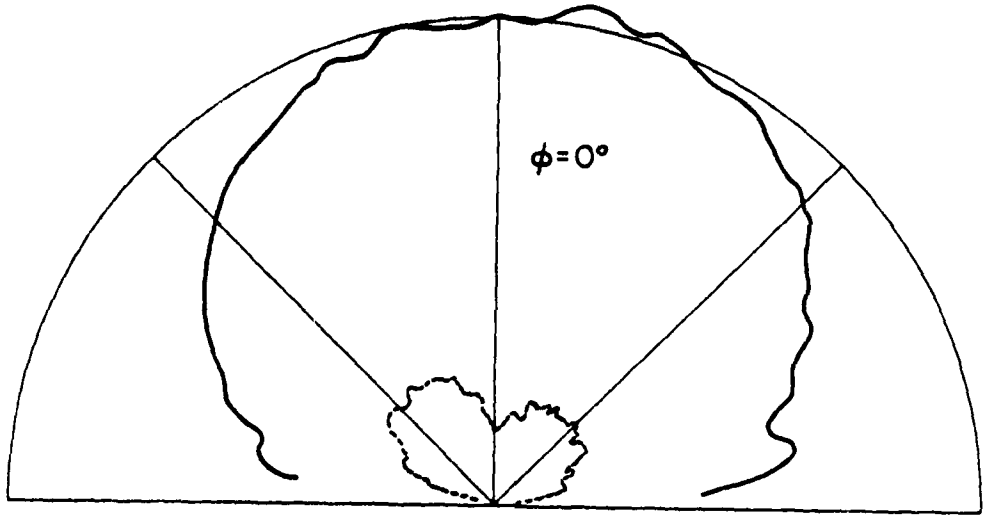

Figure 5.2 Radiation pattern in the $\phi = 0°$ plane of the disk antenna stated in Fig. 5.1 at 798 MHz (Dotted pattern is for the cross-polarized component).

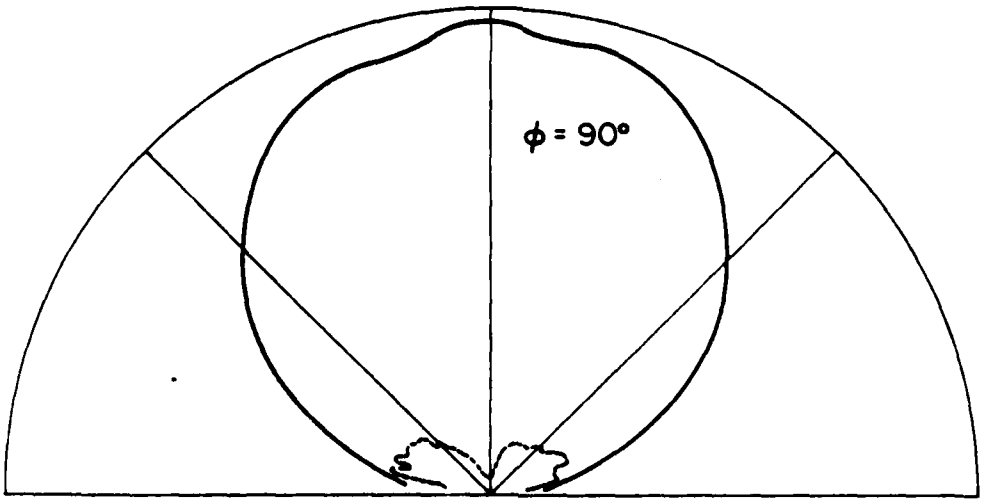

Figure 5.3. Same as in Fig. 5.2, except in $\phi = 90°$ plane.

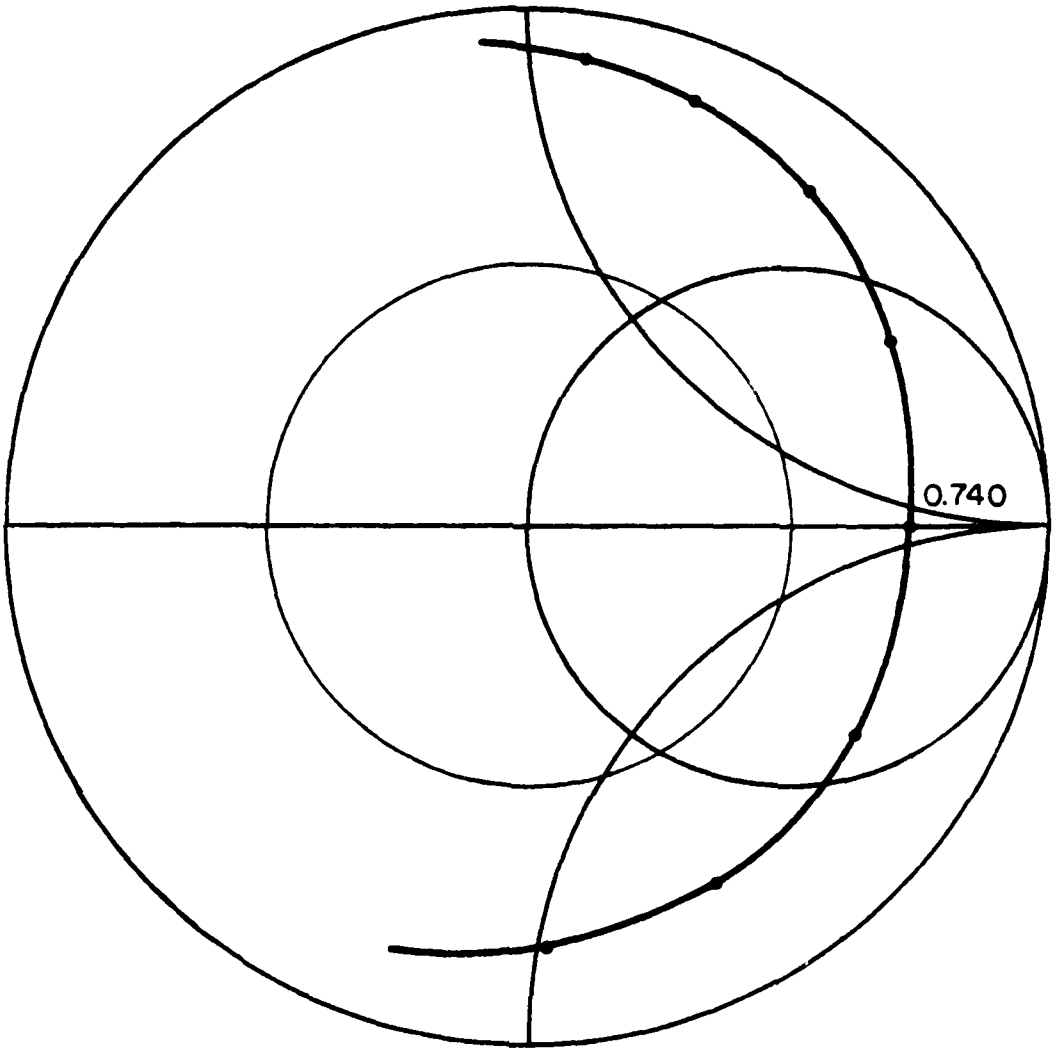

Figure 5.4. Impedance loci of an annulus microstrip antenna with radii equal to 6.63 cm and 1.77 cm fed with a cable at the outer edge.

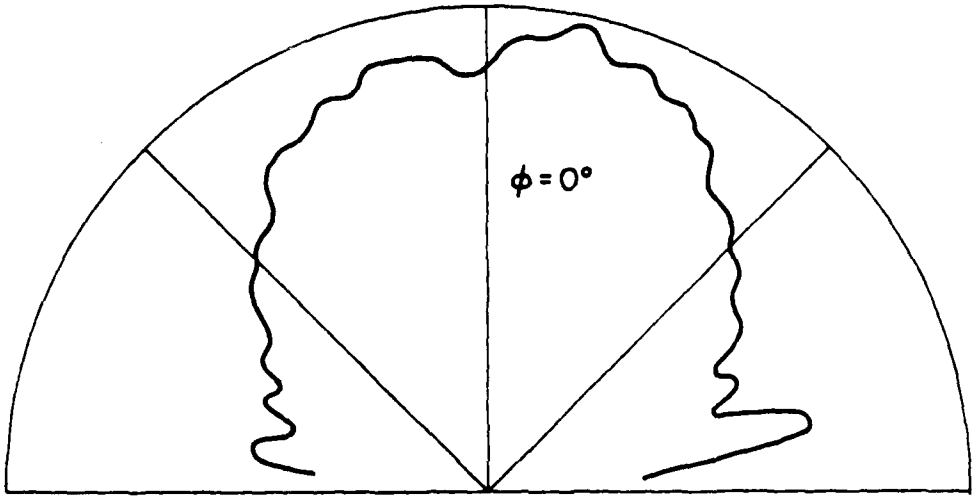

Figure 5.5. Radiation pattern in the $\phi = 0°$ plane of the annulus microstrip antenna stated in Fig. 5.4.

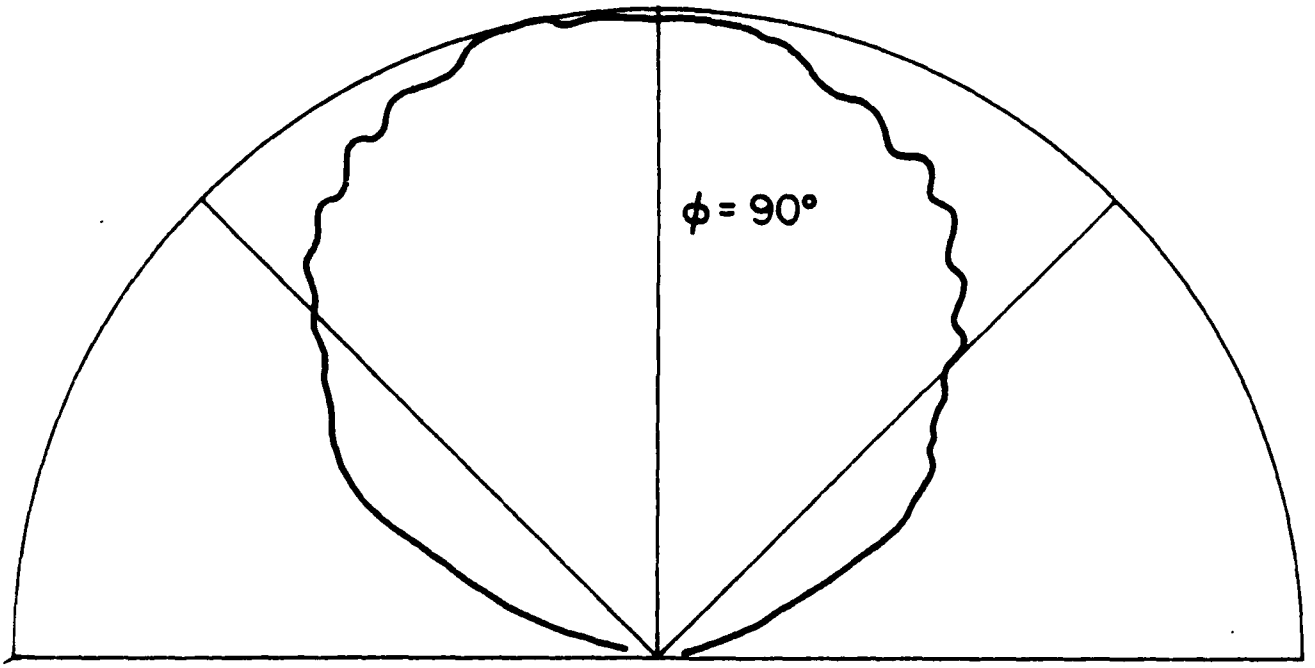

Figure 5.6. Same as in Fig. 5.5 except in $\phi = 90°$ plane.

measurements. All antennas are made of Rexolite 2200, 1/16" thick. It is seen that qualitatively they all behave nearly the same, and no one has a significantly wider bandwidth. On the other hand, this finding suggests some design flexibility for the case where a certain shape, for example rectangle, can not be made to fit a vehicle. However, the question of how the resonant frequency is related to the dimensions of the patch of a given shape can not always be easily answered.

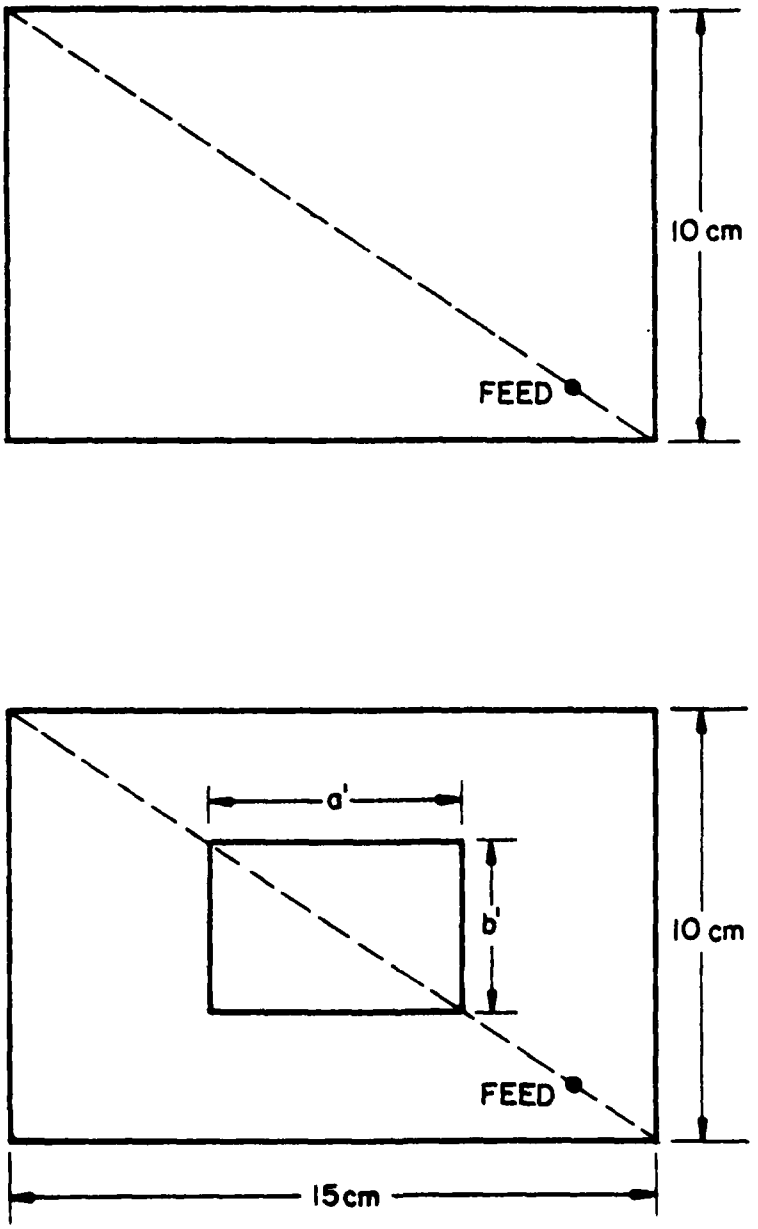

Figure 5.7. Geometry of a rectangular microstrip antenna (top) and a quadrulus (window-frame shaped) microstrip antenna (bottom) with a' = 6.0 cm, b' = 3.0 cm.

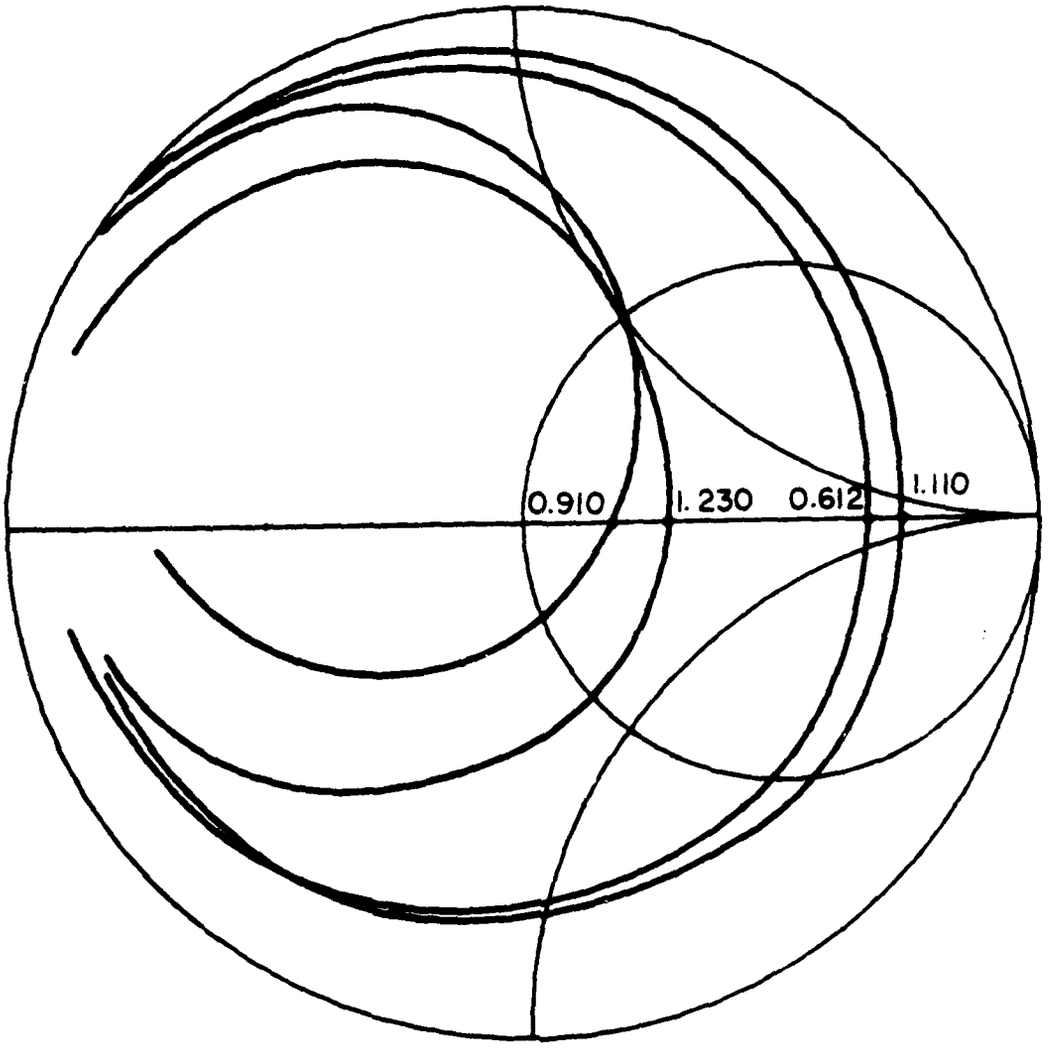

Figure 5.8. Impedance loci of the rectangular microstrip antenna shown in Fig. 5.7 for the first four modes.

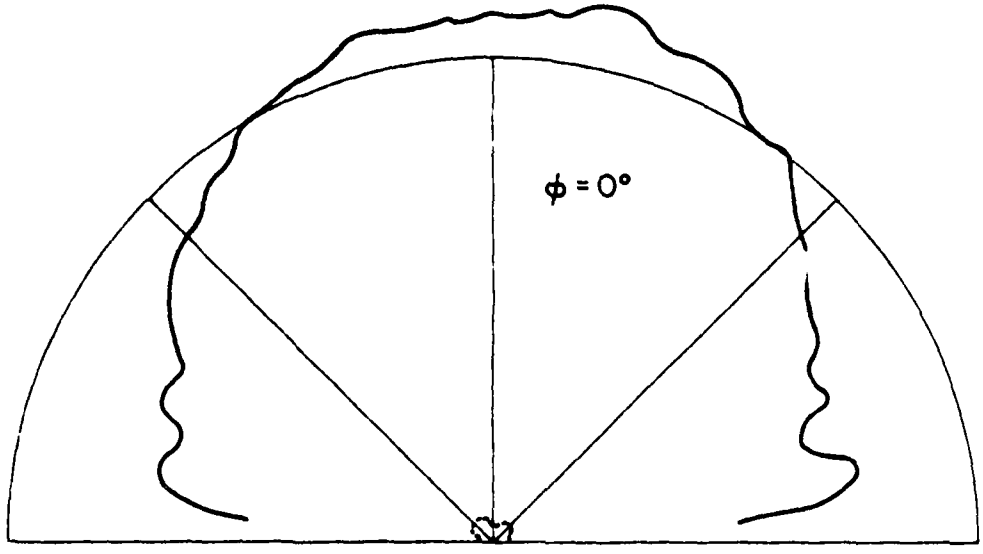

Figure 5.9. Radiation pattern in the $\phi = 0°$ plane of the rectangular microstrip antenna shown in Fig. 5.7, at 612 MHz (dotted pattern is for the cross-polarized component).

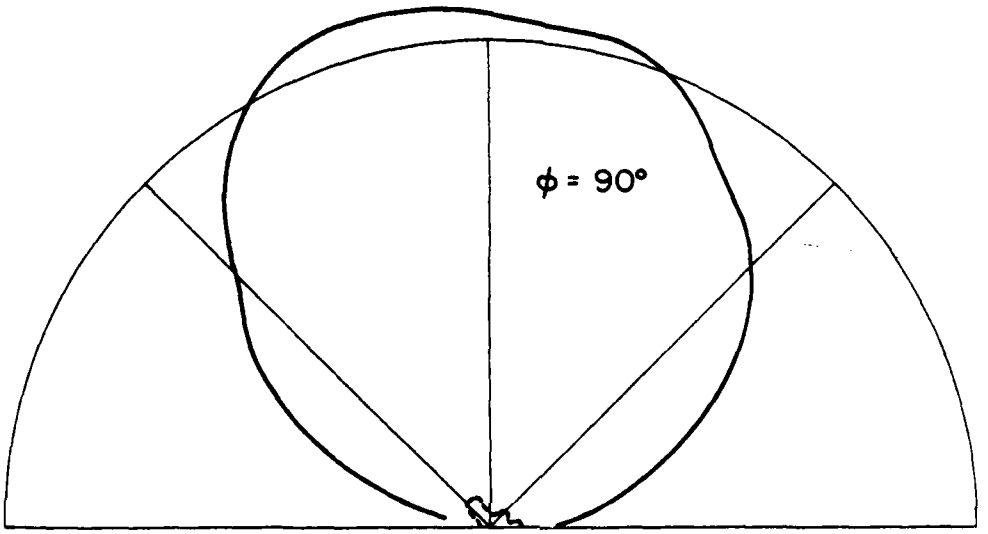

Figure 5.10. Same as in Fig. 5.9 except in $\phi = 90°$ plane.

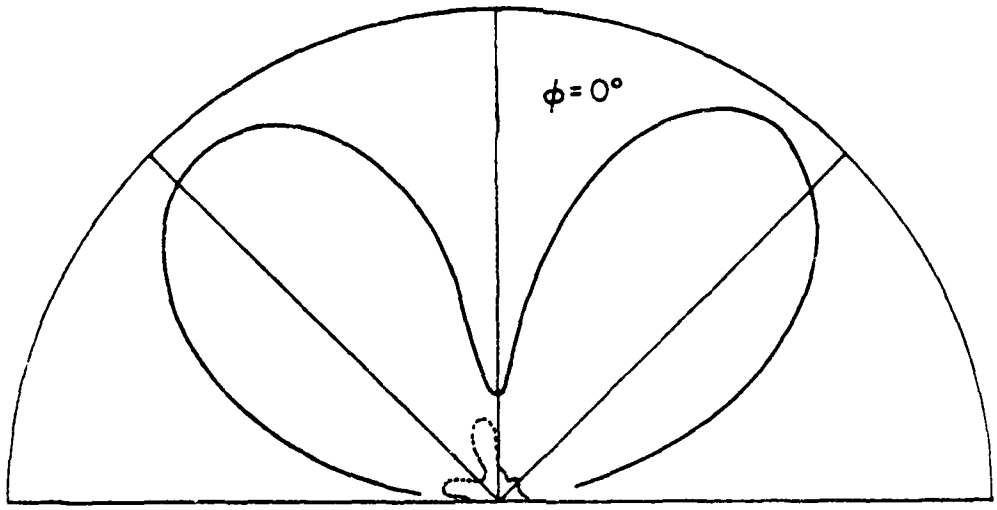

Figure 5.11. Radiation pattern in the $\phi = 0°$ plane of the rectangular microstrip antenna shown in Fig. 5.7 at 1.110 GHz (dotted pattern is for cross-polarized component).

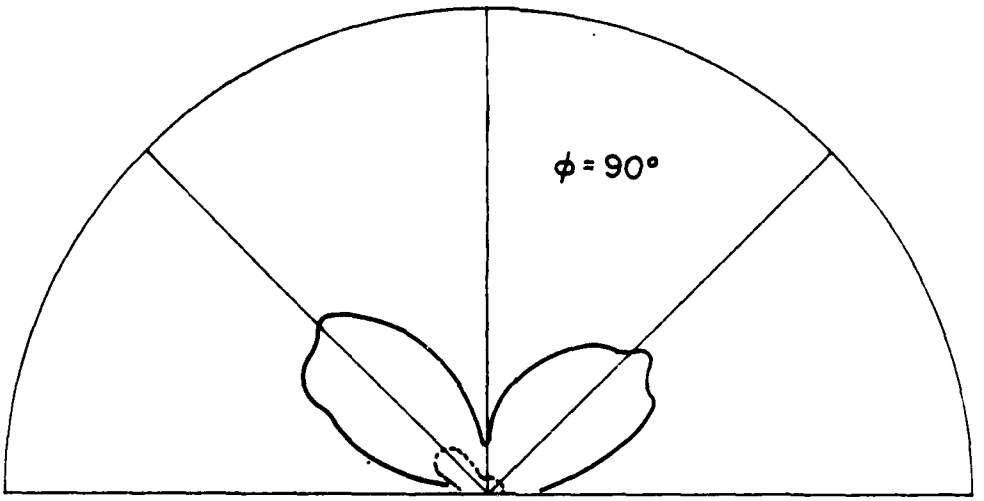

Figure 5.12. Same as Fig. 5.11 except in $\phi = 90°$ plane.

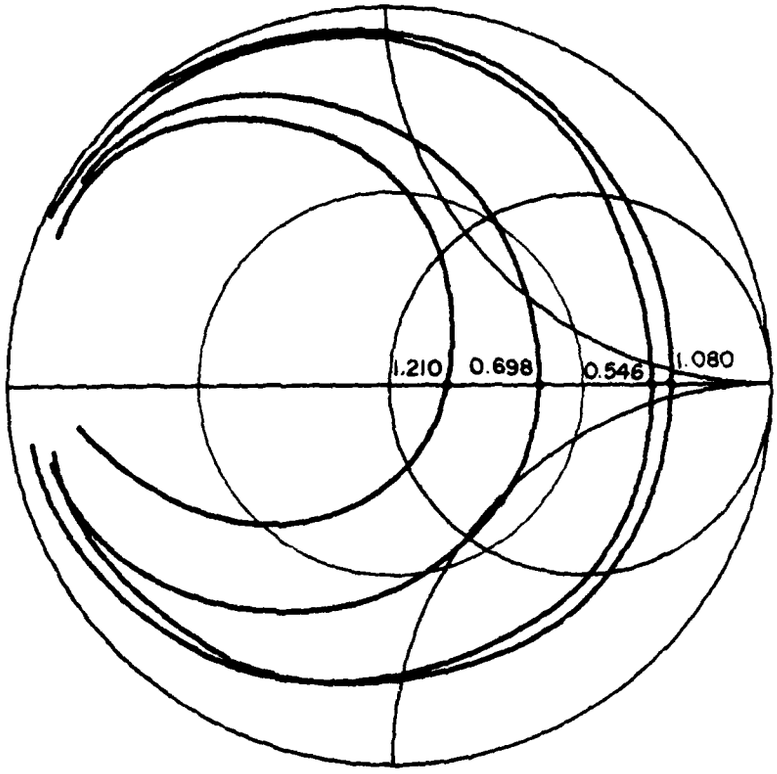

Figure 5.13. Impedance loci of a quadrulus microstrip antenna shown in Fig. 5.7 for the first four modes.

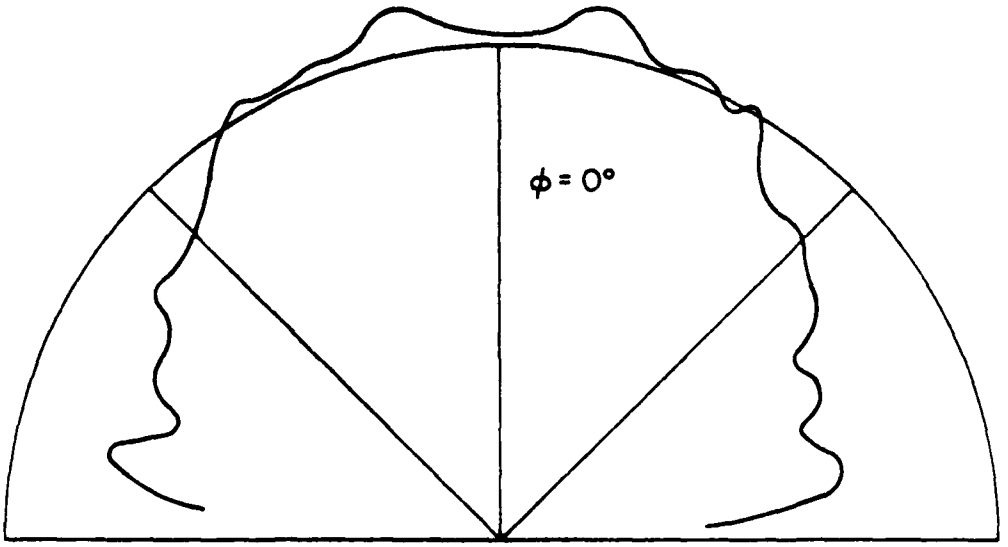

Figure 5.14. Radiation pattern in the $\phi = 0°$ plane of the quadrulus microstrip antenna shown in Fig. 5.7 at 546 MHz (dotted pattern is for cross-polarized component).

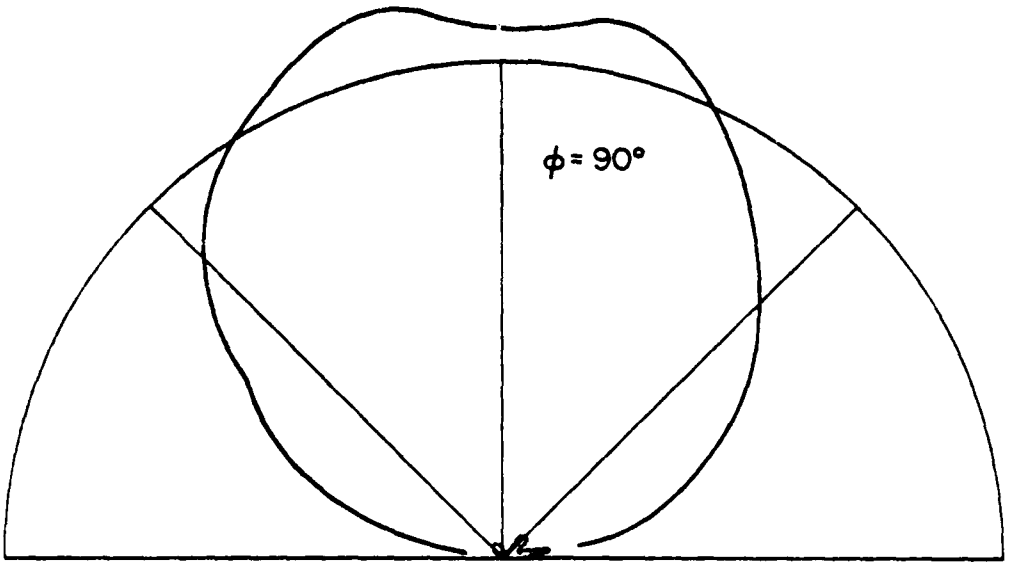

Figure 5.15. Same as Fig. 5.14 except in $\phi = 90°$ plane.

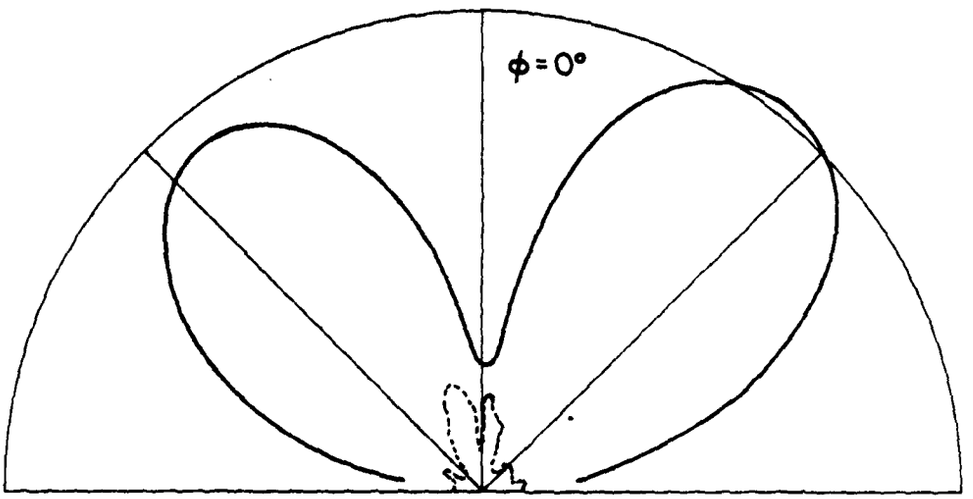

Figure 5.16. Radiation pattern in the $\phi = 0°$ plane of the quadrulus microstrip antenna shown in Fig. 5.7 at 1.080 GHz (dotted pattern is for the cross-polarized component).

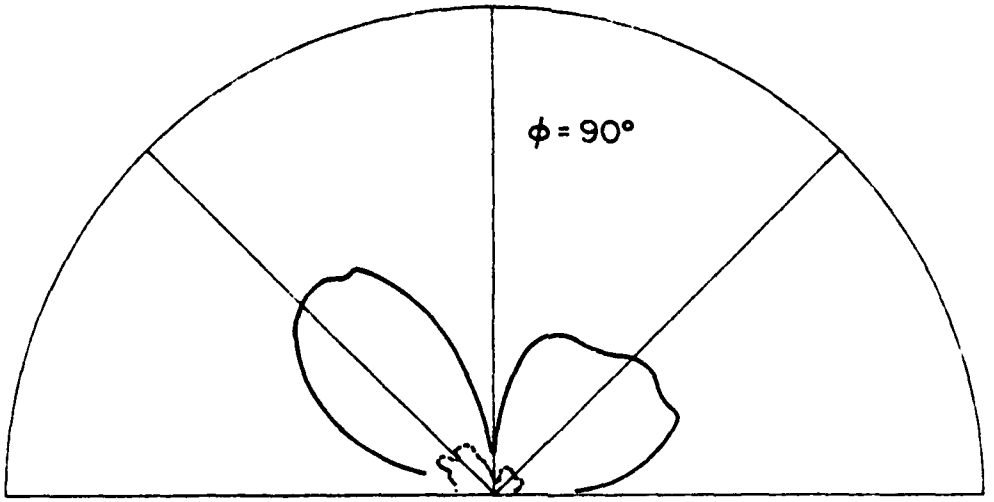

Figure 5.17. Same as Fig. 5.16 except in $\phi = 90°$ plane.

VI. STRIPLINE FEED TECHNIQUES

Microstrip antennas can be fed with a coaxial cable, a stripline, or even with a device of electric of magnetic induction. The advantages of the cable feeding are that the feed can be located anywhere in the patch (Fig. 6.1) to obtain a desired impedance characteristic and that the cable can be placed under the ground plane so that the coupling between the feed and the antenna patch is eliminated. But the disadvantage is that the structure, in contrast to the stripline feed, is not completely monolithic and becomes more difficult to produce. For this reason, an experimental investigation has been made to determine the feasability of using a stripline to feed at an interior point of the patch through a slot cut in the patch as shown in Fig. 6.1 (bottom) for three different positions. The impedance loci of this antenna are shown in Figs. 6.3 - 6.5 for various dimensions. For comparison the impedance locii of the patch fed with a cable at the same three different positions are shown in Fig. 6.2. Although they are not identical, the possibility of using stripline feed for obtaining various impedance locus is obvious.

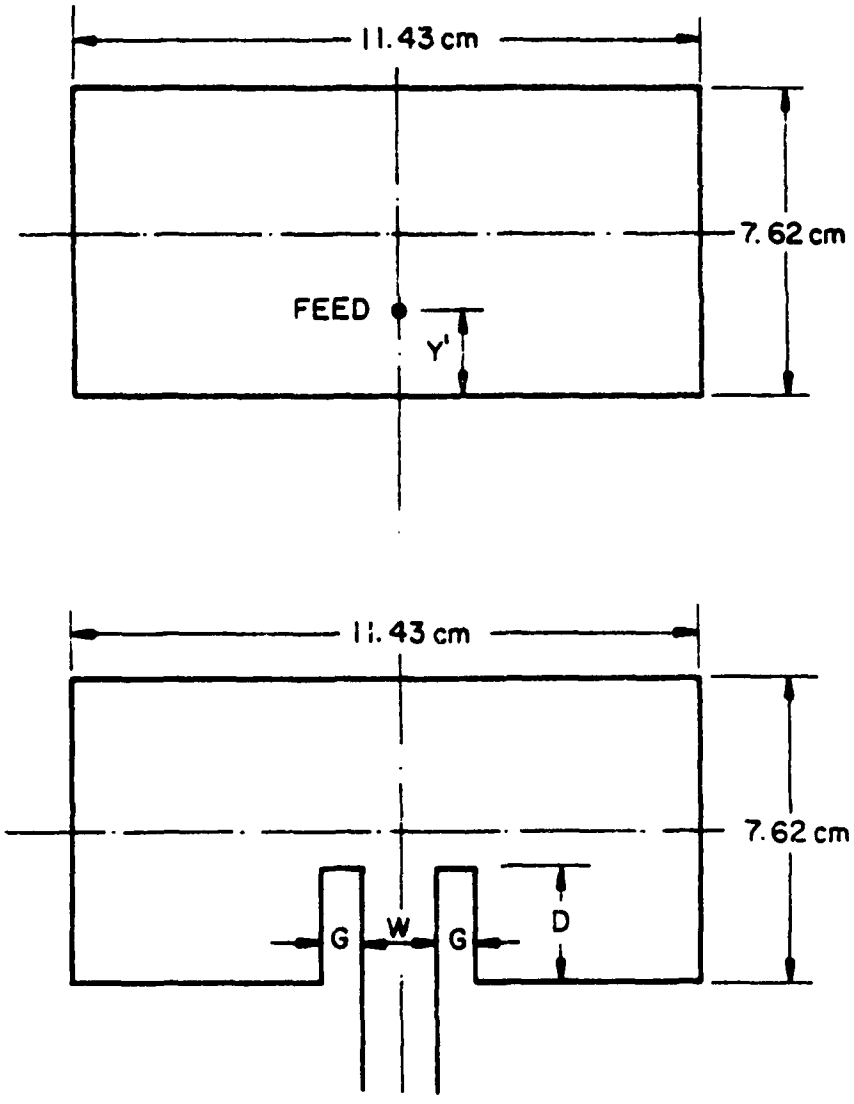

Figure 6.1. A rectangular microstrip antenna of dimensions 7.62 cm x 11.43 cm fed with a cable (top) and a stripline of width w = 0.508 cm (bottom).

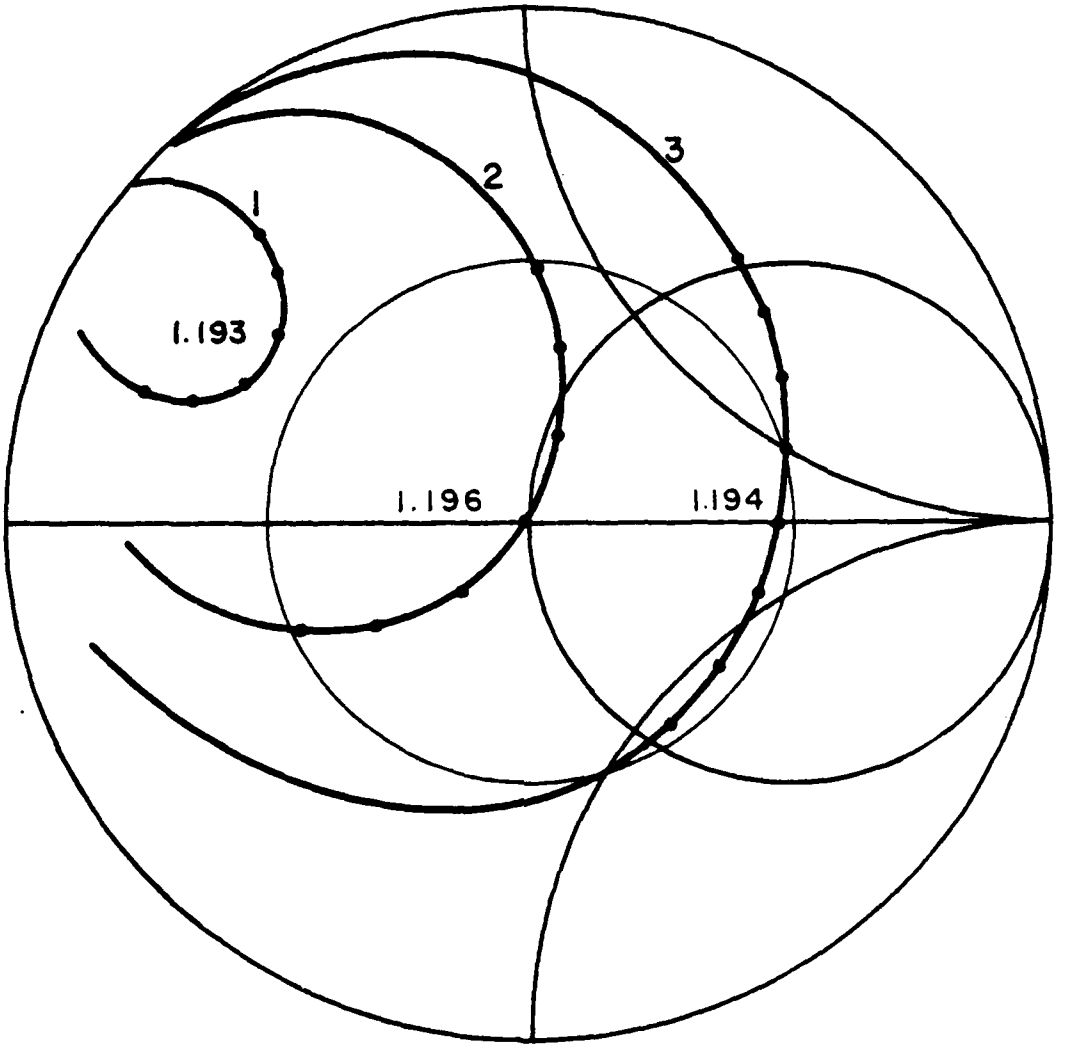

Figure 6.2. Impedance loci of the rectangular microstrip antenna fed with a cable at three different locations: (1) y' = 3.11 cm; (2) y' = 2.29 cm; and (3) y' = 0.76 cm.

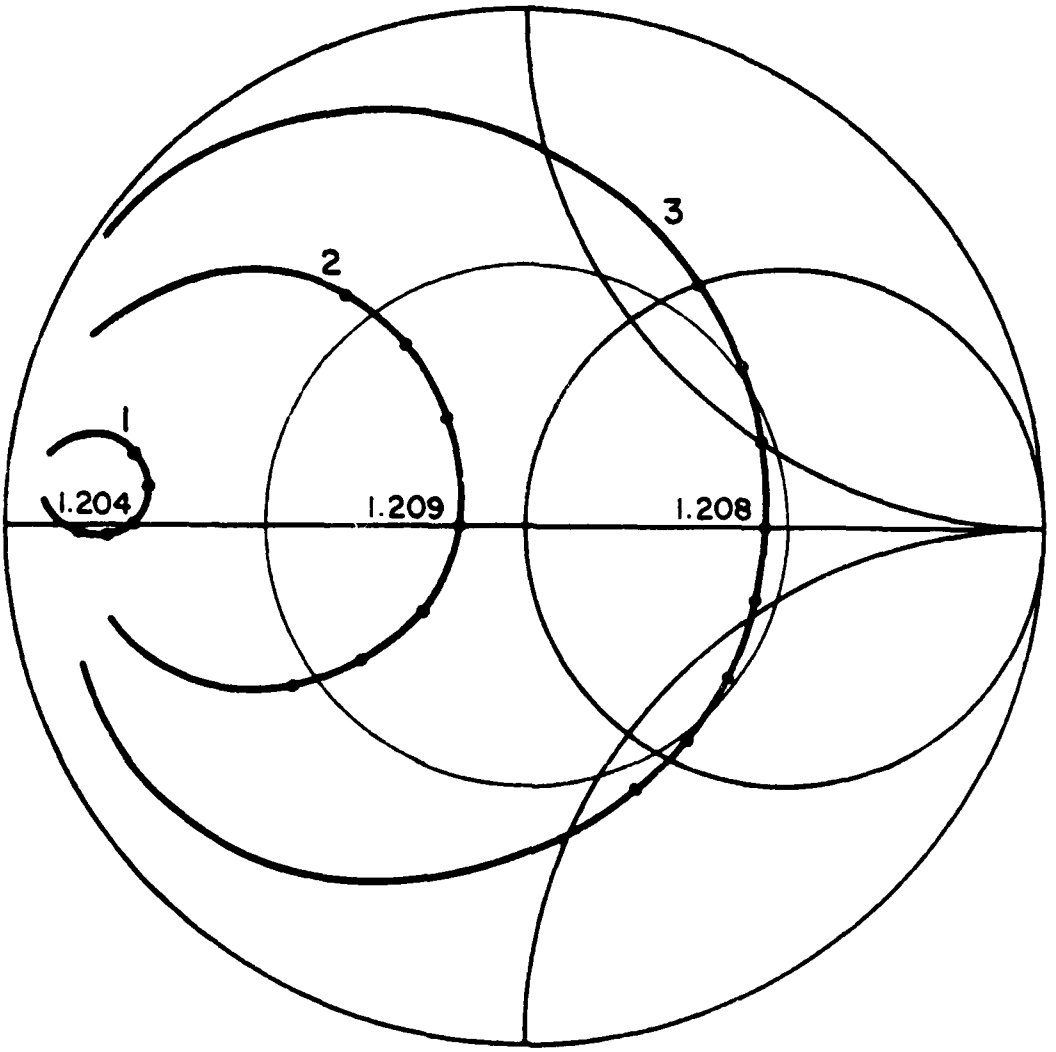

Figure 6.3. Impedance loci of a rectangular microstrip antenna fed with a stripline at three different depths: (1) D = 3.11 cm; (2) D = 2.29 cm; and (3) D = 0.76 cm, with gap G = 0.254 cm.

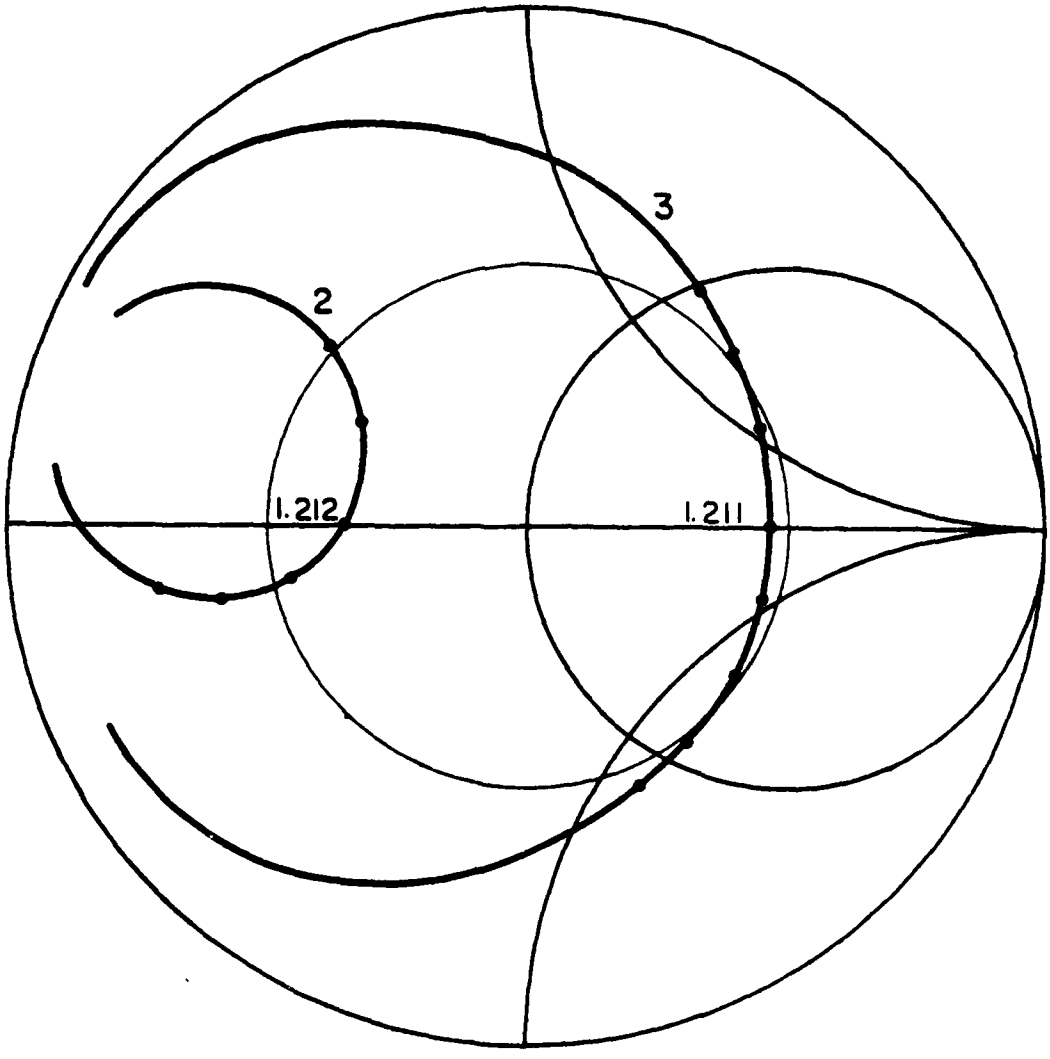

Figure 6.4. Impedance loci of a rectangular microstrip antenna fed with a stripline at two different depths: (2) D = 2.29 cm and (3) D = 0.76 cm, with Gap G = 0.559 cm. The locus for depth (1) D = 3.11 cm is too close to the $|\Gamma| = 1$ circle to be useful.

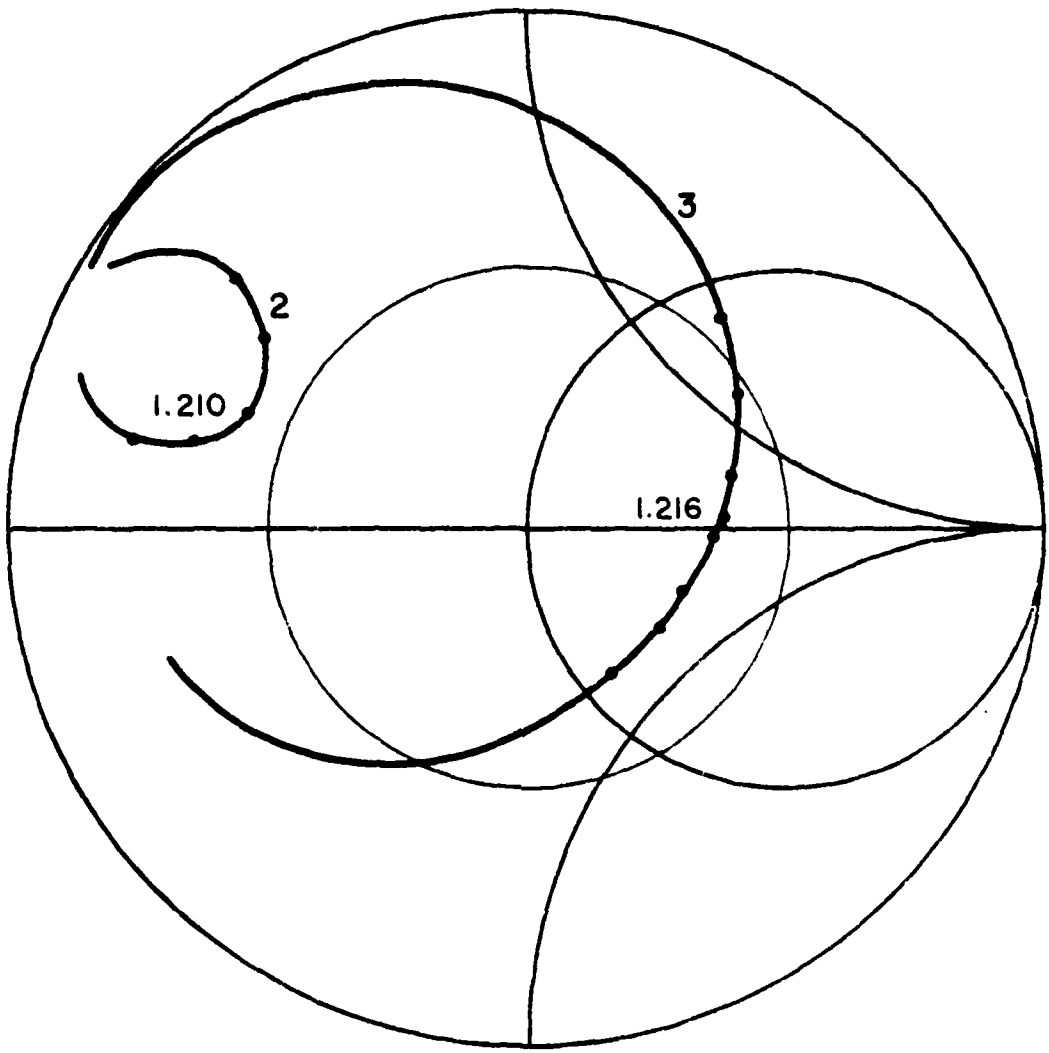

Figure 6.5. Same as Fig. 6.4 except G = 0.762 cm.

VII. EVALUATION OF LOSSES IN MICROSTRIP ANTENNA MATERIALS

Double copper cladded laminates are the most widely used material for microstrip antennas. In this material there are losses in the dielectric and losses in the copper, usually specified by the loss tangent and the conductivity, respectively. Commonly the manufacturers supply only the data of loss tangent with no mention of the copper loss. A naive user may consult a handbook for the copper conductivity for its loss, not knowing that the treatment of the copper and dielectric interface in the manufacturing process could change the effective copper loss drastically. Unfortunately, conventional methods of measurement cannot determine this loss without altering the surface condition. Therefore, a new technique is needed so that the two losses can be separated without physically separating the copper from the dielectric substrate.

Making use of the fact that the dielectric loss depends on the volume, thus the thickness of the substrate, while the copper loss on the cladding surface area, one can obtain the following simple relation:

$$\frac{1}{Q} = \frac{\Delta}{t} + \delta \tag{7.1}$$

where Q is the qualifying factor of a bona-fide cavity, made of a piece of the material with all the edges closed with copper strips; t and δ are the thickness and loss tangent of the substrate, respective; and Δ is the effective skin-depth of the copper cladding. The above equation describes a straight line in the $\Delta\delta$-plane with slope $-1/t$ and intercept $1/Q$ on the δ-axis. By constructing two or more cavities from the same material (preferrably from the same batch) but of different thickness and then measuring their Q-factors and thicknesses, one can solve for the two loss parameters Δ and δ. Various values of thickness can be obtained by stacking and clamping together two or more layers of the

material cut out from the same sheet with the interlayer copper claddings removed. In our measurement, it is observed that the value of Q-factor may vary over a small range when measurements are repeated day and night over a period of time, but does not vary significantly when the small air gap between layers are changed. The variation could be caused by the change in physical conditions, such as temperature, moisture, most probably in our case the equipment instability, etc. Because of these causes and also because of possible inhomogenieties in the material, many measurements may not yield the same values of Δ and δ. Thus, it can only be assumed that the centroid of the commonly intersected region as shown in Fig. 7.1 would be likely to give the true values. Table 2 shows the results of an extensive measurement for Rexolite 2200 at various frequencies. The conductivity calculated from them is about 3.64×10^7 mho/M, which is only 5/8 of the published conductivity of pure copper, namely 5.8×10^7 mho/M. It is found that by using this value the input impedances of many microstrip antennas,made of Rexolite 2200 and computed from the theory in Section II, agree with the measured almost exactly. This perhaps can be regarded as an independent verification of the method.

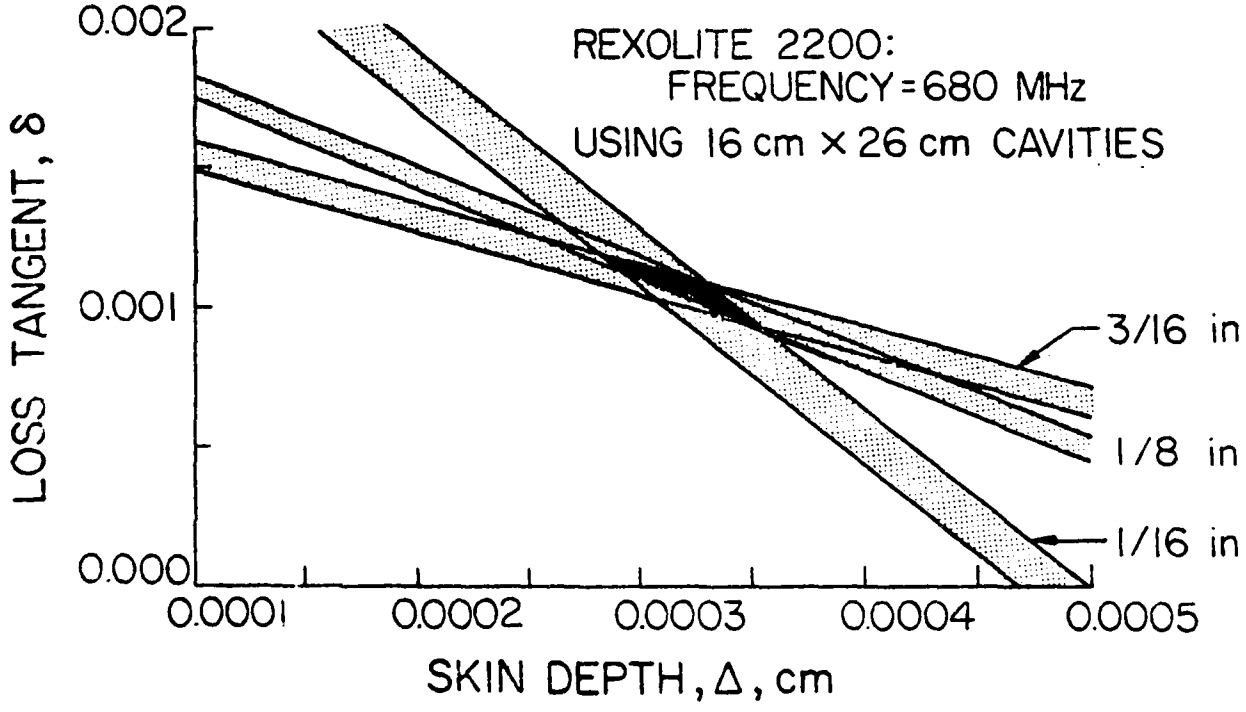

Figure 7.1. Loss tangent vs. skin depth for Rexolite 2200 with substrate thicknesses of 1/16, 1/8, and 3/16 inch.

TABLE 2. Loss tangent δ and skin depth Δ of Rexolite 2200 at various frequencies.

FIGURE	FREQUENCY MHz	δ	Δ (cm)
a	605	.00082 - .00097	.0003625 - .00039
b	680	.00097 - .00119	.00028 - .000355
c	760	.00074 - .00086	.000362 - .000385
d	820	.00078	.000366
e	865	.0007 - .00086	.000328 - .0003685
f	920	.001 - .0011	.000287 - .0003135
g	1100	.00091 - .00095	.0003 - .000313
h	1100	.00079 - .00091	.000296 - .000327
i	1365	.00098 - .00104	.000254 - .00027
j	1540	.000825- .00093	.000268 - .000299
k	1785	.00104 - .00108	.000203 - .00023
l	1940	.00084 - .00087	.000242 - .00025
m	2050	.001 - .00111	.0001865 - .000218

VIII. ARRAY STUDY

A major limitation of the microstrip antenna is narrow bandwidth, a characteristic of all resonant structure. Several attempts for broadening the bandwidth have been made by many workers [13,14] with little success. Our early trials on log-periodic arrays of microstrip elements were not successful because first it is impossible to achieve a criss-cross feed for grounded elements in order to fulfill the backfire conditions, and second an antenna does not necessarily have frequency-independent performance even if its structure satisfies the so-called scaling principle. The method of stacking two elements of slightly different dimensions have been reported [13]. A close examination of this work shows that the small increase in bandwidth so gained could have been realized more easily by using thicker substrate for a single element [see Section II, Fig. 2.5] without the complicated feeding problem as in the stacking arrangement. The obvious drawback of this approach is that the antenna is no longer thin and may protrude out of the ground plane with undesirable height. (In our previous report, it was shown that the antenna could be mounted flushly with the external ground plane. But in this arrangement, the antenna would protrude inward.) An alternative approach consists of a small array of two elements of slightly different dimensions. This is inspired by the multiple-tuning circuit for a broadband operation and has been experimentally explored by Pues, Vandensandè and van de Capelle [14]. The objective of our study is to make use of the theory discussed in Section II to systematically develop a design algorithm such that the best design will be obtained without the painstaking trial-and-error method to actually test many antennas.

A computer analysis is conducted, modeling the array elements by their equivalent networks and using the transmission line theory to calculate the

input impedance at the array feed. From this the currents at each element can be determined and then the radiation pattern of the array is calculated. The design goals are a stable pattern, good efficiency, and low SWR over a wider bandwidth than possible with a single element. In the following the network representation for the antenna element will be discussed first.

Network Representation for a Microstrip Antenna Element

The input impedance of a microstrip antenna element can be represented conveniently in a Foster expansion. To illustrate this, consider a rectangular patch discussed in Section II, where it was shown that for input current of 1 amp,

$$Z = V/I = j\omega\mu_0 t \sum_{m,n=0}^{\infty} \frac{\phi_{mn}^2(x',y')}{k_{mb}^2 - k^2} j_0^2\left(\frac{m\pi d}{2a}\right) \quad . \tag{8.1}$$

Let

$$\omega_{mn} = ck_{mn}/\sqrt{\varepsilon_r} \quad ,$$

$$c = 3 \times 10^8 \text{ m/s} \quad ,$$

$$\alpha_{mn} = \frac{\mu_0 t c^2}{\varepsilon_r} \phi_{mn}^2(x',y') \; j_0\left(\frac{m\pi d}{2a}\right) , \tag{8.2}$$

$$G_{mn}(\omega) = \omega\delta/\alpha_{mn} , \tag{8.3}$$

$$C_{mn} = 1/\alpha_{mn} , \tag{8.4}$$

$$L_{mn} = \alpha_{mn}/\omega_{mn}^2 . \tag{8.5}$$

Then Equation (8.1) can be written in a more interesting form:

$$Z = \sum_{m,n=0}^{\infty} \frac{1}{G_{mn}(\omega) + j\omega C_{mn} - j/\omega L_{mn}} \quad . \tag{8.6}$$

As microstrip antennas are narrow band devices, for operation in the frequency band of, say, mode (M,N), $G_{mn}(\omega)$ can be replaced by $G_{mn}(\omega_{M,N})$. In doing so, Eq. (8.6) represents a Foster expansion of the input impedance function of a network consisting of an infinite number of parallel resonant circuit in series. Furthermore, since L_{mn} decreases with increasing modal indices, the infinite number of high order Foster sections can simply be combined to form a single inductance in series with the remaining circuit elements as shown in Fig. 8.1a.

In case that the antenna is operating near a resonant frequency ω_{MN} which is well separated from all other resonant frequencies, a further simplification of the network representation is possible, as shown below:

$$Z \approx \frac{1}{G_{MN}(\omega_{MN}) + j\omega C_{MN} - j/\omega L_{MN}} + j\omega L' \tag{8.7}$$

where

$$L' = \sum_{m,n\neq M,N} \frac{\alpha_{mn}}{\omega_{mn}^2 - \omega_{MN}^2} \tag{8.8}$$

This is simply the impedance of a parallel resonant circuit in series with an inductance L' as shown in Fig. 8.1b, and this also explains why the impedance locus is shifted to the inductive region.

Two Element Array

Two rectangular patch elements of slightly different dimensions are considered. As reported previously [5], the mutual coupling effect between two elements is not significant unless they are unusually close. Thus, in general the array design is essentially a circuit problem since each element can be adequately represented by a circuit in Fig. 8.1b with impedance given by Eq. (8.7). What requires is mainly the feed network design. To keep the

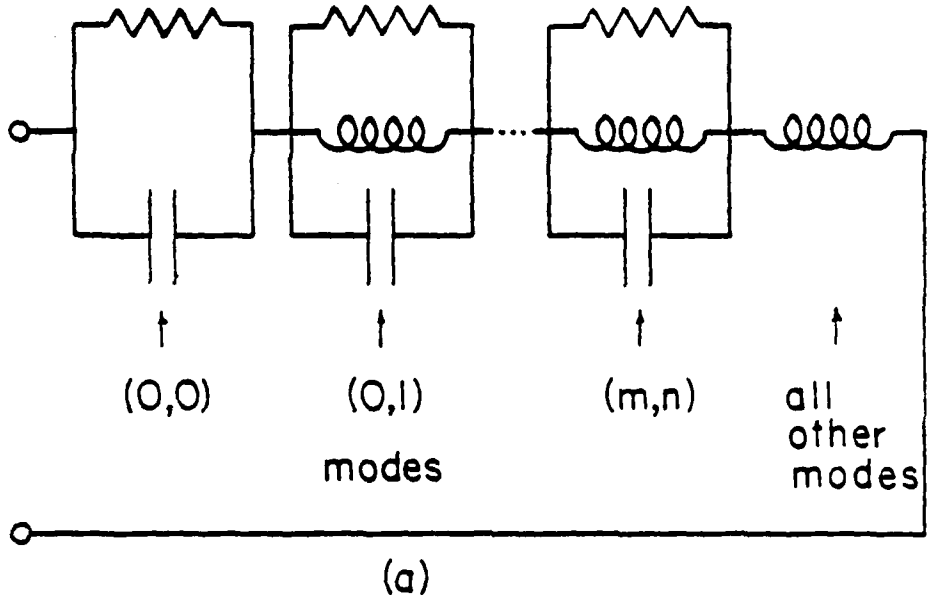

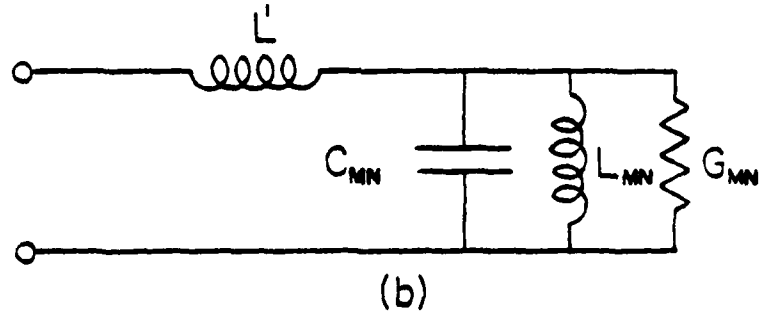

Figure 8.1 Circuit representations for microstrip antenna.
(a) General network representation for frequency band about a resonant mode.
(b) A simplified representation for the band about the resonant frequency of (M,N)th mode when it is well separated from all others.

structure monolithic, simple stripline feed is considered as shown in Fig. 8.2 The relative excitation currents to the elements as well as the input impedance at the array feed point can thus be expressed in terms of the dimensions of each patch (a and b), feed location to each element, and the feed network parameters, namely the line length d and line width W for each of three line sections. Once the currents are found the radiation pattern and the efficiency of the array can be computed. A computer program is written to evaluate all these quantities. The following few parameters are chosen a priori: the substrate thickness t of the material is 0.15 cm; the line width is determined for a 50-ohm characteristic impedance; the patch dimensions are chosen to resonate at two adjacent frequencies, for example, 795 MHz and 805 MHz. By observing the impedance locus and radiation pattern as the line lengths $d^{(1)}$, $d^{(2)}$, and $d^{(3)}$ are varied, hopefully we can obtain an optimum design.

Before searching for the optimum design, the theory as well as the computer program are checked against the experiment. A typical result is shown in Fig. 8.3. The agreement is only fair. Considerable effort has been expended to determine the possible causes of the discrepancy. This is found partly due to the discontinuities of the striplines and the stripline-to-coax connector at the feed point, and mostly due to the inaccuracy of our equipment which is over fifteen years old. Inhomogeneity in the material, and in accuracy in the construction are also possible contributing factors. However, the computer program seems to be capable of at least predicting the general behavior of the array.

The computer program is finally used to search for the best design. Unfortunately, it is found that the case for a broadband in impedance characteristics doe not give a stable pattern over the band (i.e., the beam may tilt from one side to the other). It is a simple matter to use our program to evaluate the two element array reported by Pues, Vandersande, and van de Capelle [14]. The result shows that the beam is skewed from the broadside by

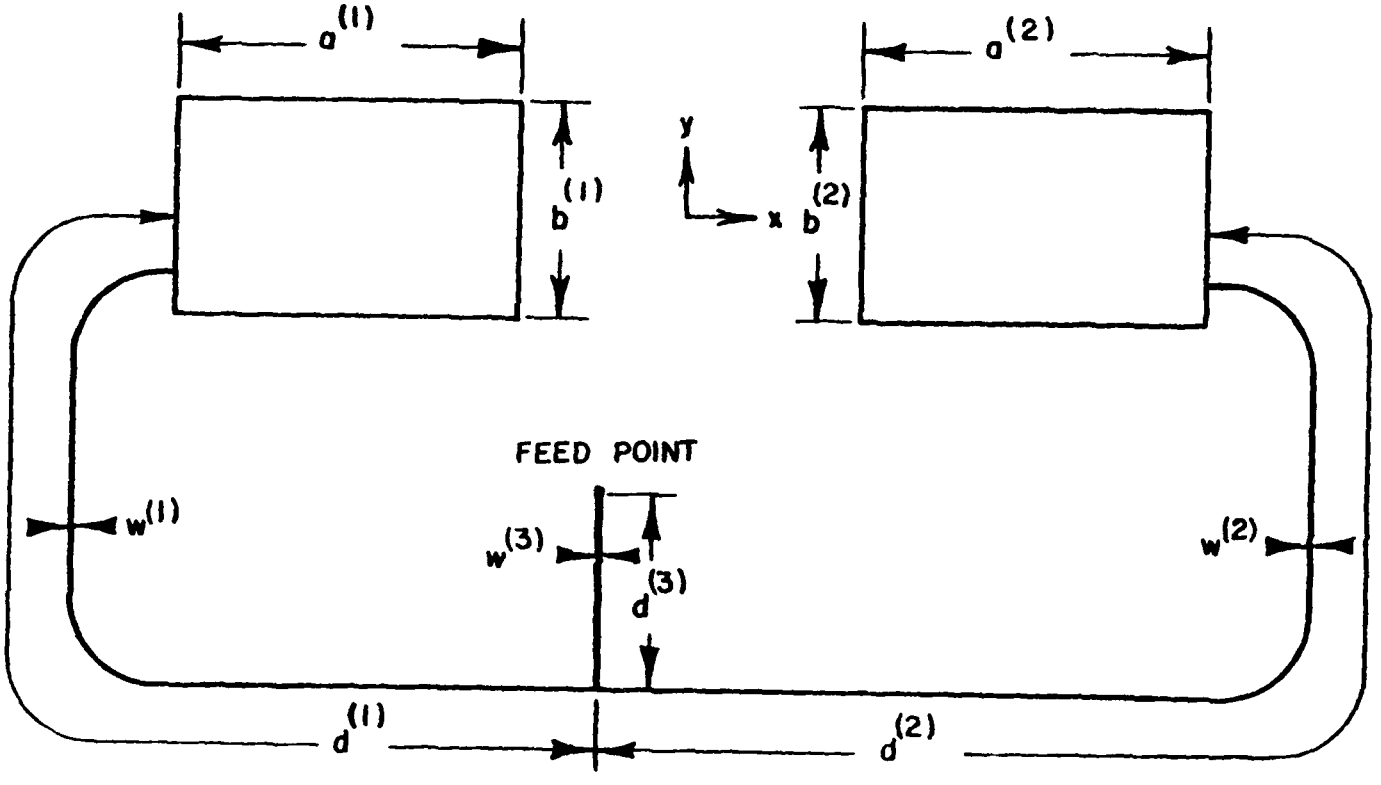

Figure 8.2. Geometry of a two-element array.

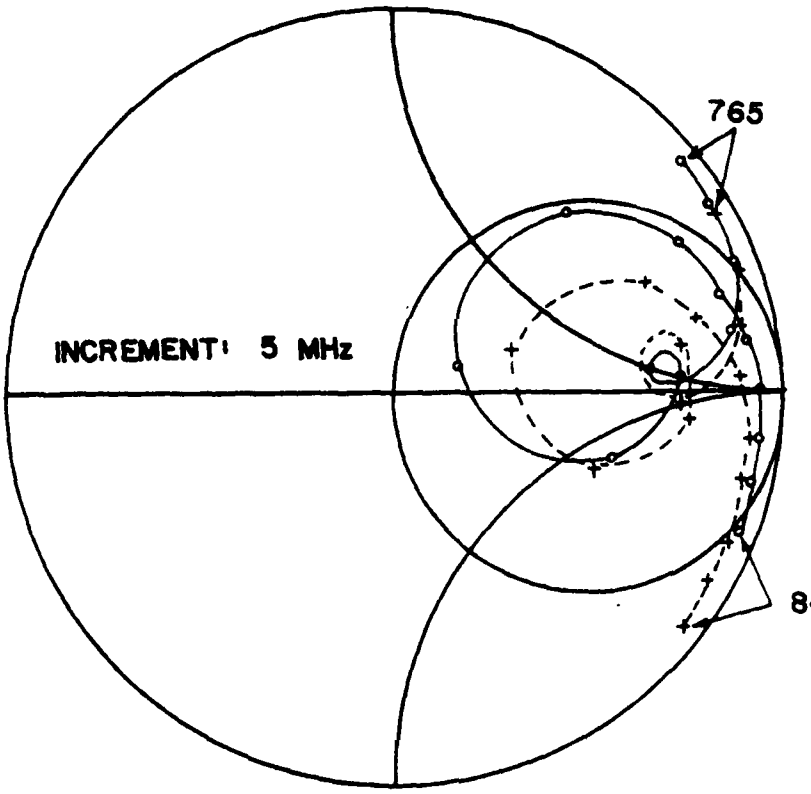

+---------+ COMPUTED POINTS

o———————o MEASURED LOCUS

$f_o^{(1)}$ = 795 MHz, $f_o^{(2)}$ = 805 MHz,

$Q^{(1)}$ = 90, $Q^{(2)}$ = 91, D_e = 23·6 cm,

$d^{(1)}$ = 49·8 cm, $d^{(2)}$ = 64·5 cm, $d^{(3)}$ = 9·31 cm,

$w^{(1)} = w^{(2)} = w^{(3)}$ = 0·44 cm, t = 0·15 cm,

l = 0·0036 cm

Figure 8.3. Measured and computed impedance loci of the two-element array.

a considerable amount. Therefore, their claim of wide bandwidth is not substantiated. Although our attempt to broaden the bandwidth of a two-element array is not completely successful, it is believed the computer program could be used for the design of an array for dual, or even multiple frequency operation. It is further believed that the program can be expanded to study symmetrical arrays of three or more elements in which case a stable pattern could be maintained.

IX. GENERAL THEORY AND INFINITE ARRAY

Early interest of the microstrip antennas has been focused on their compactness in structure, and the investigations are therefore mostly confined to thin substrates. Taking advantage of this special property one is able to develop a simple theory based on the cavity model which turns out to be surprisingly accurate. As in the development of all scientific studies, progress and inventions are often made by extending one's knowledge to new situations. It is therefore natural to expand our investigation to "thick" microstrip antennas, or to microstrip antennas to be operated at much higher frequencies. From our investigation this appears to be the only effective way to broaden the bandwidth. It seems that this purpose alone justifies a major effort to develope a general theory for microstrip antennas.

If the substrate is not sufficiently thin, the assumption of vanishing transverse E-components and vanishing longitudinal H-component with respect to the normal of the patch is no longer valid, and it follows that the cavity model with a magnetic wall along the patch perimeter would fail. One is therefore forced to formulate the problem on the satisfaction of the following conditions: (a) the boundary conditions on the patch and ground plane; (b) the field continuity condition over the air-dielectric interface, and (c) the source condition at the feed. The last condition is often overlooked by many workers. In formulating the problem in this manner one finds that it is closely related to that of an infinite periodic array of microstrip elements. As stated before, mutual coupling between microstrip elements, at least for moderately thin substrate, is generally not strong; therefore, the input impedance of any element in the array will approach that of a single isolated element as element spacing increases. This provides another approach to the single element problem; in fact, numerically speaking, this approach appears to be somewhat simpler.

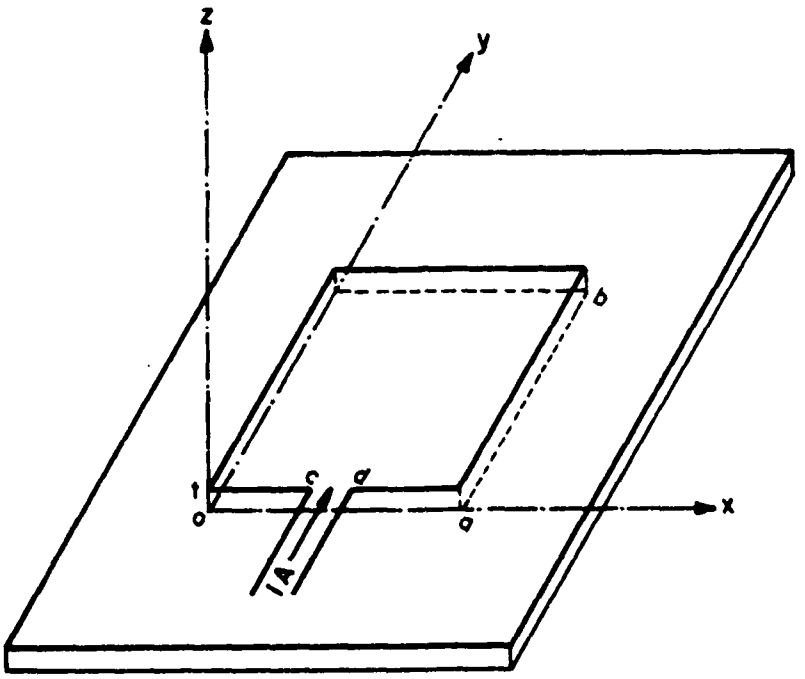

Figure 9.1. Geometry of a rectangular microstrip antenna fed with a stripline at y = 0, x = c to d.

During the course of this contract, the two problems just stated have been studied off and on. Because of the numerical complication, no quick solution is anticipated. The purpose is to make some preliminary study which hopefully will lead to a more vigorous investigation in the next contract period.

Simple Element

We shall consider a rectangular element of dimensions a x b. There are several ways to incorporate the source condition into the formulation. At present we assume a stripline feed at the y = 0 edge with an input current of 1 amp distributed over the line width x = c to x = d as shown in Fig. 9.1. Let the current density on the patch be $\hat{x}f_x(x,y) + \hat{y}f_y(x,y)$ and its Fourier transform be $\hat{x}F_x(p,q) + \hat{y}F_y(p,q)$. Then the following set of integral equations for $F_x(p,q)$ and $F_y(p,q)$ can be obtained:

$$\frac{j}{4\pi^2} \iint_{-\infty}^{\infty} F_y(p,q)(e^{-jpd} - e^{-jpc})/p \; dpdq = 1$$

$$\iint_{-\infty}^{\infty} [G_{xx}(p,q)\; F_x(p,q) + G_{yx}(p,q)\; F_y(p,z)]\; e^{-jpx-jqy}\; dpdq = 0$$

$$\iint_{-\infty}^{\infty} [G_{xy}(p,q)\; F_x(p,q) + G_{yy}(p,q)\; F_y(p,q)]\; e^{-jpx-jqy}\; dpdq = 0$$

$$\text{for } 0 \leq x \leq a \quad , \quad 0 \leq y \leq b$$

where

$$G_{xy}(p,q) = G_{yx}(p,q) = \frac{pqD_3}{k_0^2 D_1 D_2}$$

$$G_{xx}(p,q) = \frac{p^2 D_3 - k_0^2 D_1}{k_0^2 D_1 D_2}$$

$$G_{yy}(p,q) = \frac{q^2 D_3 - k_0^2 D_1}{k_0^2 D_1 D_3}$$

$$D_1 = s' - j\varepsilon_r s \cot s't$$

$$D_2 = s - js \cot s't$$

$$D_3 = s' - js \cot s't$$

$$s = (k_0^2 - p^2 - q^2)^{1/2}$$

$$s' = (\varepsilon_r k_0^2 - p^2 - q^2)^{1/2}$$

This set of integral equations can only be solved numerically. An initial attempt has been made, but the computation appears to be so involved that a major effort is needed.

Infinite Periodic Array

Consider a periodic array of infinite number of rectangular patch elements, each having the same dimensions and excitations as before, and all arranged in rectangular lattices with periodicity A and B along the x-and y-axis, respectively. Assume that all elements are fed in phase and the current in any one element to be $\hat{x}J_x(x,y) + \hat{y}J_y(x,y)$. Since the current must also be periodic with period A and B along the x- and y-axis, it can be expanded in Fourier series with coefficients:

$$\begin{matrix} F_x \\ y \end{matrix}(m,n) = \iint_{AxB} \begin{matrix} J_x \\ y \end{matrix}(x,y)\, e^{-j\xi_m x - j\eta_n y}\, dxdy$$

where

$$\xi_m = 2\pi m/A \quad , \quad \eta_n = 2\pi n/B \quad ,$$

$$a < A \quad , \quad b < B \quad .$$

Since $J_y(x,0) = 1/(d - c)$ for $c < x < d$,

$$F_y(m) = \int_{x=c}^{d} e^{-j\xi_m x}\, dx$$

$$= (e^{-j\xi_m d} - e^{-j\xi_m d})/\xi_m$$

After applying the boundary conditions, the following two equations for $F_x(m,n)$ and $F_y(m,n)$ are obtained:

$$\sum_{m,n} [F_x(m,n)\, G_{xx}(m,n) + F_y(m,n)\, G_{yx}(m,n)]\, e^{j\xi_m x + j\eta_n y} = 0 \quad ,$$

$$\sum_{m,n} [F_x(m,n)\, G_{xy}(m,n) + F_y(m,n)\, G_{yy}(m,n)]\, e^{j\xi_m x + j\eta_n y} = 0 \quad ,$$

$$\text{for } 0 \leq x \leq a \quad , \quad 0 \leq y \leq b \quad ,$$

where all G-functions are the same as before if p and q are replaced by ξ_m and η_n, respectively. Comparing the above set of equations with that for the simple element, one notices the close similarity. But the summations being denumerable, from numerical point of view, it seems to be simpler to consider the infinite array problem first. It could be solved approximately by enforcing the equality of these equations at a sufficient number of points (x_i, y_i) for the equal number of the truncated unknowns $F_x(m,n)$ and $F_y(m,n)$. Alternatively, one can assume $J_x(x,y)$ and $J_y(x,y)$ be expressed in terms of a set of judiciously chosen basis functions and then solve for their expansion coefficients. Some simple basis functions have been investigated but are found not suitable because of the convergence problem. But this initial effort has provided us with much information and experience on the numerical aspect of the problem. This investigation should certainly be continued.

X. REFERENCES

1. R. E. Munson, "Conformal microstrip antennas and microstrip phased arrays," IEEE Trans. Antennas Propagat., AP-22, pp. 74-78, Jan. 1974

2. A. G. Derneryd, "Linearly polarized microstrip antennas," IEEE Trans. Antennas Propagat., AP-24, pp. 846-851, Nov. 1976.

3. R. F. Harrington, Time Harmonic Electromagnetic Fields, p. 276, McGraw-Hill, New York.

4. P. K. Agrawal and M. C. Bailey, "An analysis technique for microstrip antennas," IEEE Trans. Antennas Propagat., AP-25, pp. 756-759, Nov. 1977.

5. Y. T. Lo, et. al, "Study of microstrip antennas, microstrip phased arrays, and microstrip feed networks," Tech. Report RADC-TR-77-406, Oct. 1977, A053005.
Also, Y. T. Lo, D. Solomon, and W. F. Richards, "Theory and experiment on microstrip antennas," IEEE Trans. Antennas Propagat., AP-27, pp. 137-145, Mar. 1979.

6. Y. T. Lo, W. F. Richards, and D. D. Harrison, "An improved theory for microstrip antennas and applications--Part I," Interim Report RADC-TR-79-111, May, 1979. A paper based on this work will appear in IEEE Trans. Antennas Propagat., Jan. 1981, A070791.

7. Y. T. Lo, D. D. Harrison, and W. F. Richards, "An analysis of disc microstrip antenna--Part II," Interim Report RADC-TR-79-132, May 1979, A070794.

8. J. L. Kerr, "Microstrip polarization techniques," Proceedings of the 1978 Antenna Applications Symposium, Sept. 1978.

9. L. C. Shen, "The elliptical microstrip antenna with circular polarization, to appear in IEEE Trans. Antennas Propagat.
S. A. Long and L. C. Shen, "The circularly polarized elliptical printed-circuit antenna," IEEE AP-S International Symposium Digest, pp. 731-734, June, 1980.

10. Private communication by S. A. Long

11. Y. T. Lo, P. S. Simon, and W. F. Richards, "A study of microstrip antenna elements and arrays," Interim Report, RADC (to appear) 1980.

12. I. P. Yu, "Low profile circularly polarized antennas," NASA Report, N78-15332, 1978.

13. P. S. Hall, C. Wood, and C. Garrett, "Wide bandwidth microstrip antennas for circuit integration," Electronics Letters, Vol. 15, pp. 458-459, 19 July 1979.

14. H. Pues, J. Vandensande, and A. Van de Capelle, "Broadband microstrip resonator antennas," IEEE AP-S International Symposium Digest, pp. 268-271, May 1978.

15. D. H. Schaubert, F. G. Farrar, A. R. Sindoris, and S. T. Hayes, "Frequency agile microstrip antennas," IEEE AP-S International Symposium Digest, pp. 601-604, June 1980.

MISSION
of
Rome Air Development Center

RADC plans and executes research, development, test and selected acquisition programs in support of Command, Control Communications and Intelligence (C^3I) activities. Technical and engineering support within areas of technical competence is provided to ESD Program Offices (POs) and other ESD elements. The principal technical mission areas are communications, electromagnetic guidance and control, surveillance of ground and aerospace objects, intelligence data collection and handling, information system technology, ionospheric propagation, solid state sciences, microwave physics and electronic reliability, maintainability and compatibility.

Printed by
United States Air Force
Hanscom AFB, Mass. 01731